Strong-coupling expansion of chiral models

Massimo Campostrini, Paolo Rossi, and Ettore Vicari

Dipartimento di Fisica dell'Università and INFN, I-56126 Pisa, Italy

(Received 8 February 1995)

The strong-coupling character expansion of lattice models is reanalyzed in the perspective of its complete algorithmization. The geometric problem of identifying, counting, and grouping together all possible contributions is disentangled from the group-theoretical problem of weighting them properly. The first problem is completely solved for wide classes of spin models admitting a character-like expansion and for arbitrary lattice connectivity. The second problem is reduced to the evaluation of a class of invariant group integrals defined on simple graphs. Since these integrals only depend on the global symmetry of the model, results obtained for principal chiral models can be used without modifications in lattice gauge theories. By applying the techniques and results obtained we study the two-dimensional principal chiral models on the square and honeycomb lattice. These models are a prototype field theory sharing with QCD many properties. Strong-coupling expansions for Green's functions are derived up to 15th and 20th order, respectively. Large-N and $N = \infty$ results are presented explicitly. Related papers are devoted to a discussion of the results.

PACS number(s): 11.15.Me, 11.15.Ha, 11.15.Pg

I. INTRODUCTION

It is certainly appropriate to consider two-dimensional principal chiral models as a theoretical physics laboratory. These models display a rich physical structure, and share with four-dimensional gauge theories a number of fundamental properties: non-Abelian symmetry with fields in the matrix representation, asymptotic freedom, and dynamical mass generation. Moreover, principal chiral models admit a $1/N$ expansion and a large-N limit which is a sum over planar diagrams, in total analogy with non-Abelian gauge theories.

However, the absence of local gauge invariance and the reduced number of dimensions make chiral models much simpler to handle both by analytical and by numerical methods. Moreover, the on-shell solution of the models is known by Bethe ansatz methods: A factorized S matrix exists and the particle spectrum is explicitly known. We can therefore try to make progress, both in analytical and in numerical techniques, by testing these methods on chiral models and, in case of success, applying them to four-dimensional gauge theories.

The spirit of this approach is well expressed in the papers by Green and Samuel [1–3], who advocated a systematic study of lattice chiral models as a preliminary step towards an understanding of lattice gauge theories, especially in the large-N limit. One of the techniques favored by the above-mentioned authors was the strong-coupling character expansion. However, the existence of a large-N phase transition from the strong- to weak-coupling phase seemed to indicate at that time an obstruction to further pushing this method of investigation.

In much more recent times, a few facts came to suggest that this "no-go" result might be overpessimistic. It was indeed observed by the present authors [4–6] that scaling of physical observables is present in finite-N chiral models already in a coupling region within the convergence radius of the strong-coupling expansion. Moreover, a change of variables corresponding to adopting the so-called "energy scheme" for the definition of the temperature smoothens the lattice β function to the point that asymptotic scaling is observed within the strong-coupling region. These patterns are unaffected by growing N, and therefore survive the large-N phase transition. These "experimental" observations led us to reconsider the possibility that a strong-coupling approach could be turned into a predictive method for the evaluation of physical quantities in the neighborhood of the continuum fixed point of the models.

A second theoretical motivation for a renewed effort towards extending strong-coupling series of chiral models, especially for large N, comes in connection with the possibility that the above-mentioned transition, while uninteresting for standard continuum physics, may be related to a description of quantum gravity by the so-called "double scaling limit" [7–10]. In simple models, this limit is studied by analytical techniques, but more complex situations might need perturbative methods, and strong-coupling seems well suited for such an analysis, which corresponds to exploring the region in the vicinity of the first singularity in the complex coupling constant plane.

Another significant change, of a completely different nature, has occurred since the original studies on the strong-coupling character expansion (cf. Ref. [11] for a review) were performed. The increased availability of symbolic-manipulation computer programs and the enormous increase in the performance of computers have now made the strong-coupling expansion a plausible candidate for an algorithmic implementation, which might extend series well beyond the level that can be reached by purely human resources, while granting a definitely higher reliability of results.

The purpose of the present work is to set the stage and make a significant effort towards a complete algo-

STRONG-COUPLING EXPANSION OF CHIRAL MODELS

rithmization of the strong-coupling character expansion.

Two major classes of problems must be handled and solved. The first has to do with counting the multiplicities of terms appearing in the expansion. It is basically a geometrical problem and it leads to the definition of a "geometrical factor." We must stress the fact that this geometrical factor depends only on the lattice connectivity, and therefore applies without any modification to the strong-coupling expansion of spin models admitting a characterlike expansion, including $O(N)$ models with nearest-neighbor interactions [12]. We have completely solved this problem, with no conceptual restrictions on the dimensionality and connectivity of the lattice. We have not addressed the corresponding problem for lattice gauge theories, but we are confident that no major conceptual obstruction should arise in pursuing that program.

The second class of problems is related to the evaluation of group integrals that appear as coefficients of the expansion. Evaluating group integrals is an algebraic problem, and in principle a solved one. However, algorithmic implementation is not in practice a trivial task, and therefore we limited ourselves to a general classification and to an explicit evaluation of the cases of direct interest to our calculations, with a few useful generalizations. We stress that the evaluation of "group-theoretical factors" is universal, and results may be applied as they stand to lattice gauge theories.

The representation of the strong-coupling expansion in terms of explicitly evaluated geometrical factors and symbolically denoted group-theoretical factors can be achieved by a fully computerized approach, and applies as it stands to wide classes of nonlinear σ models defined on group manifolds. This is probably the main result of the present paper. However, we shall not exhibit here the explicit general formulas resulting from our approach, because they are so long that their practical use does necessarily involve computer manipulation; therefore we shall make available our results in form of computer files.[1]

The application of our results to $O(N)$ models is definitely simpler than the case discussed here, since the evaluation of group-theoretical factors lends itself to a completely algorithmic implementation. The corresponding results will be presented in a forthcoming paper.

The techniques presented here can be applied with minor changes to higher-dimensional spin models. The computation of geometrical factors for three-dimensional spin models is in progress, and results for principal chiral models and $O(N)$ models will be presented in forthcoming papers.

The present paper is organized as follows.

In Sec. II we review the character expansion, fix our notation, and present some useful formulas.

In Sec. III we outline the procedure of the expansion by identifying the logical steps and defining the relevant geometrical and algebraic objects entering the computation. Among these we introduce the basic notion of a *skeleton diagram*, whose multiplicity is the geometrical factor and whose connected value, or *potential*, is the group-theoretical factor. In Sec. IV we explain how one may algorithmically evaluate the geometrical factor. In Sec. V we introduce the problem of computing the group-theoretical factor. Section VI is devoted to some technical remarks on group integration. Section VII offers some details on the computation of potentials for principal chiral models. In Sec. VIII we analyze the main features of the strong-coupling expansion of the two-point fundamental Green's functions, introducing a parametrization for the propagator in the case of a two-dimensional square lattice. In Sec. IX we discuss the relevant features of the honeycomb lattice, and we present a few results for physical quantities.

Appendix A is devoted to a presentation of some of our results concerning the explicit evaluation of potentials. Appendix B is a list of potentials ordered according to their appearance in the strong-coupling expansion. Appendix C is a presentation of our results for large but finite N in the square-lattice formulation of the models. Appendix D clarifies some nonstandard features of honeycomb-lattice models using the Gaussian model as a guide. Appendix E is the same as Appendix C for the honeycomb-lattice formulation.

The present paper is the first of a series of papers devoted to the strong-coupling analysis of two-dimensional lattice chiral models. In a second paper we will present our analysis of the large-N strong-coupling series by series-resummation techniques, while a third paper will be devoted to a comparison with Monte Carlo studies of the large-N critical behavior.

II. CHARACTER EXPANSION: GENERALITIES

The strong-coupling expansion of field theories involving matrix-valued fields and enjoying $G \times G$ group symmetry is best performed applying the character expansion, which reduces the number of contributions to a given order in the expansion and decouples the geometrical counting of configurations from the group-theoretical factor.

The whole subject is reviewed in detail in Ref. [11], and we recall here only those properties that are essential in order to make our presentation as far as possible self-contained. We shall only discuss the symmetry groups $G = U(N)$: Extensions to $SU(N)$ can be achieved following Ref. [1] and applying the results presented in Ref. [5].

In the theory described by the lattice action

---

[1] Publicly available by anonymous ftp on the host `ftp.difi.unipi.it`, in the directory `pub/campo/StrongCoupling`.

$$S_L = -N\beta \sum_{x,\mu} \left[\mathrm{Tr}\{U(x)\,U^\dagger(x{+}\mu)\} + \mathrm{Tr}\{U(x{+}\mu)\,U^\dagger(x)\} \right], \tag{1}$$

the character expansion is achieved by replacing the Boltzmann factors with their Fourier decomposition

$$\exp\left\{N\beta\left[\mathrm{Tr}\{U(x)\,U^\dagger(x{+}\mu)\} + \mathrm{Tr}\{U(x{+}\mu)\,U^\dagger(x)\}\right]\right\} = \exp\{N^2 F(\beta)\} \sum_{(r)} d_{(r)}\tilde{z}_{(r)}(\beta)\,\chi_{(r)}\left[U(x)\,U^\dagger(x{+}\mu)\right], \tag{2}$$

where

$$F(\beta) = \frac{1}{N^2}\ln\int dU \exp\{N\beta(\mathrm{Tr}\,U + \mathrm{Tr}\,U^\dagger)\} = \frac{1}{N^2}\ln\det I_{j-i}(2N\beta) \tag{3}$$

is the free energy of the single-matrix model, $\sum_{(r)}$ denotes the sum over all irreducible representations of G, $\chi_{(r)}(U)$ and $d_{(r)}$ are the corresponding characters and dimensions, respectively, and I_{j-i} ($i,j = 1,...,N$) is an $N{\times}N$ matrix of modified Bessel functions. We recall here the orthogonality relations for representations:

$$\int dU \mathcal{D}_{ab}^{(r)}(U)\,\mathcal{D}_{cd}^{(s)\,*}(U) = \frac{1}{d_{(r)}}\delta_{(r),(s)}\,\delta_{a,c}\,\delta_{b,d}, \qquad \chi_{(r)}(U) = \mathcal{D}_{aa}^{(r)}(U). \tag{4}$$

In U(N) groups, (r) is characterized by two sets of decreasing positive integers $\{l\} = l_1,...,l_s$, $\{m\} = m_1,...,m_t$, and we define the order n of (r) by

$$n = n_+ + n_-, \quad n_+ = \sum_{i=1}^{s} l_i, \quad n_- = \sum_{j=1}^{t} m_j. \tag{5}$$

We may define the ordered set of integers $\{\lambda\} = \lambda_1,...,\lambda_N$ by the relationships

$$\begin{aligned}
\lambda_k &= l_k, \quad k \le s, \\
\lambda_k &= 0, \quad s < k < N - t + 1, \\
\lambda_k &= -m_{N-k+1}, \quad k \ge N - t + 1.
\end{aligned} \tag{6}$$

It is then possible to write down explicit representations of all characters and dimensions:

$$\chi_{\{\lambda\}}(U) = \frac{\det\left|\exp\{i\phi_i(\lambda_j + N - j)\}\right|}{\det\left|\exp\{i\phi_i(N - j)\}\right|}, \tag{7}$$

$$d_{\{\lambda\}} = \frac{\prod_{i<j}(\lambda_i - \lambda_j + j - i)}{\prod_{i<j}(j - i)} = \chi_{\{\lambda\}}(1), \tag{8}$$

where ϕ_i are the eigenvalues of the matrix U. As a consequence, it is possible to evaluate explicitly the character coefficients $\tilde{z}_{(r)}$ by the orthogonality relations

$$\begin{aligned}
d_{\{\lambda\}}\tilde{z}_{\{\lambda\}} &= \int dU \exp\{N\beta(\mathrm{Tr}\,U + \mathrm{Tr}\,U^\dagger)\}\chi_{\{\lambda\}}(U) \\
&\quad \times \exp\{-N^2 F(\beta)\} \\
&= \frac{\det I_{\lambda_i + j - i}(2N\beta)}{\det I_{j-i}(2N\beta)}.
\end{aligned} \tag{9}$$

Equation (9) becomes rapidly useless with growing N, due to the difficulty of evaluating determinants of large matrices. It is, however, possible to obtain considerable simplifications, in the strong-coupling regime and for sufficiently large N, when we consider representations such that $n < N$. In this case, character coefficients are simply expressed by [1]

$$d_{\{l;m\}}\tilde{z}_{\{l;m\}} = \frac{1}{n_+!}\frac{1}{n_-!}\sigma_{\{l\}}\sigma_{\{m\}}(N\beta)^n\left[1 + O(\beta^{2N})\right], \tag{10}$$

where we have introduced the quantity $\sigma_{\{l\}}$, the dimension of the representation $l_1,...,l_s$ of the permutation group, enjoying the property

$$\int \chi_{\{l\}}(U)(\mathrm{Tr}\,U^\dagger)^p dU = \sigma_{\{l\}}\delta_{p,n_+}. \tag{11}$$

It is important to notice that the strong-coupling expansion and the large-N limit do not commute: Large-N character coefficients have jumps and singularities at $\beta = \frac{1}{2}$ [1], and therefore the relevant region for a strong-coupling character expansion is $\beta < \frac{1}{2}$.

A consequence of Eq. (10) is the relationship

$$z \equiv \tilde{z}_{1;0}(\beta) = \beta + O(\beta^{2N+1}), \tag{12}$$

and, in turn, because of the property

$$z(\beta) = \frac{1}{2}\frac{\partial}{\partial\beta}F(\beta), \tag{13}$$

one may obtain the large-N relationship

$$F(\beta) = \beta^2 + O(\beta^{2N+2}). \tag{14}$$

According to the above observations, at $N = \infty$ the relationship $F = \beta^2$ may only hold when $\beta < \frac{1}{2}$, even if the function β^2 is perfectly regular for all β.

For the purpose of actual computations it is convenient to have expressions in closed form for the quantities $\sigma_{\{l\}}$ and $d_{\{l;m\}}$ not involving infinite sums or products even in the $N \to \infty$ limit. We found such expressions in the form

$$\frac{1}{n_+!}\sigma_{l_1,...,l_s} = \frac{\prod_{1 \le j < k \le s}(l_j - l_k + k - j)!}{\prod_{i=1}^{s}(l_i + s - i)!} \tag{15}$$

and a similar relationship for $\sigma_{\{m\}}$. Notice that these quantities are independent of N. Now by manipulating appropriately Eq. (8) we can show that

$$d_{\{l;m\}} = \frac{\sigma_{\{l\}}}{n_+!} \frac{\sigma_{\{m\}}}{n_-!} C_{\{l;m\}} \, , \qquad (16)$$

where

$$C_{\{l;m\}} = \prod_{i=1}^{s} \frac{(N-t-i+l_i)!}{(N-t-i)!} \prod_{j=1}^{t} \frac{(N-s-j+m_j)!}{(N-s-j)!}$$

$$\times \prod_{i=1}^{s} \prod_{j=1}^{t} \frac{N+1-i-j+l_i+m_j}{N+1-i-j} \, . \qquad (17)$$

The essential feature of Eq. (17) is the possibility of extracting results with a finite number of operations even in the large-N limit. As a by-product we obtain the large-N character coefficients in the useful form

$$\frac{\tilde{z}_{\{l;m\}}}{z^n} \to \frac{N^n}{C_{\{l;m\}}} \, . \qquad (18)$$

III. OUTLINE OF THE PROCEDURE

The general purpose of the strong-coupling expansion is an evaluation of the Green's functions of the model as power series in β. If we are interested in the mass spectrum of the model, we may focus on the class of two-point Green's functions defined by

$$G_{(r)}(x) = \frac{1}{d_{(r)}} \left\langle \chi_{(r)} \left[U^\dagger(x) U(0) \right] \right\rangle , \qquad (19)$$

and even more specifically we may decide to evaluate the fundamental two-point Green's function

$$G(x) = \frac{1}{N} \left\langle \text{Tr} \left[U^\dagger(x) U(0) \right] \right\rangle . \qquad (20)$$

Evaluating such expectation values by the character expansion involves performing the group integrations that are generated from choosing an arbitrary representation for each link of the lattice. As a consequence of Eq. (10), only a finite number of nontrivial representations contribute to any definite order in the series expansion of $G(x)$ in powers of β; we must, however, find a systematic way of identifying the relevant contributions.

As a preliminary condition for the definition of an algorithmic approach to the strong-coupling expansion of $G(x)$, it is convenient to identify explicitly all the logical steps of such a computation and define a number of objects that play a special role in it.

A. Assignments

Each lattice integration variable $U(y)$ can only appear in the integrand either through the representation characters defined on links terminating on the lattice site y or through the observable whose expectation value is to be evaluated. According to the rules of group integration, nontrivial contributions are obtained only if the product of all representations involving $U(y)$ contains the identity (the trivial representation).

We define an *assignment* $\{r\}$ to be a choice of a representation for each link of the lattice that is consistent with the above requirement. Necessary conditions for an assignment can be obtained by a close examination of the rules for the composition of two irreducible representations of U(N). When we consider Green's functions in the class defined by Eq. (19), we recognize that the operator whose expectation value we are evaluating, when considered from the point of view of group integration, plays the role of a unit length link connecting the sites x and 0, weighted by a factor $d_{(r)}^{-2}$. Therefore all the relevant group integrals can be put into correspondence with integrals appearing in the character expansion of the partition function (possibly in higher dimensions).

Changing the convention for the orientation of links changes each representation r into its conjugate $\bar{r}$ ($l \leftrightarrow m$), but, since $\tilde{z}_{(r)} = \tilde{z}_{(\bar{r})}$, it does not affect the expansion. Hence we can consider all links terminating in a given site as "ingoing." It is now possible to prove that an assignment must satisfy the following conditions at each lattice site:

$$\sum_i (n_+^i - n_-^i) = 0, \qquad (21)$$

$$n_\pm^j \le \sum_{i \ne j} n_\mp^i \quad \text{(nonbacktracking condition)}, \qquad (22)$$

where the summation is extended to all ingoing links.

Order by order in the strong-coupling expansion, the relevant assignments involve nontrivial representations only on a finite number of links, which allows the possibility of drawing on the lattice the *diagram* of each assignment. Such a diagram is characterized by vertices, where more than two nontrivial representations meet, and paths, i.e., chains of links connecting vertices. Orthogonality of representations implies that the choice of representation along a given path cannot change. We will denote the length of each path p by L_p, and the corresponding (nontrivial) representation by r_p. The topology $\mathcal{S}$ of a diagram may be represented by the connectivity matrix between its vertices. As we shall show later, the value of the group integral associated with each assignment can only be a function of r_p, L_p, and $\mathcal{S}$; we shall denote it by $R_{\{r,L\}}^{(\mathcal{S})}$.

B. Configurations

The set (n_+, n_-) does not in general identify uniquely a representation. It is convenient to define *oriented configurations*: They are the sets of all assignments having the same (n_+^l, n_-^l) for each link of the lattice. The relevance of oriented configurations in the context of the strong-coupling expansion stays in the fact that they are in a one-to-one correspondence with the monomials one would obtain in the integrand after the series expansion of the Boltzmann factor in powers of β. They are therefore the simplest objects admitting a meaningful definition for their connected contributions.

Equation (10) tells us that the lowest-order contribution of any character coefficient to the strong-coupling

series depends only on $n = n_+ + n_-$. Hence it is useful to define (unoriented) *configurations* by summing up all the oriented configurations characterized by the same value of n_l for each link of the lattice. The set $\{n\} = (n_1, ...)$ uniquely identifies a configuration. We might have defined configurations directly as the sets of all assignments sharing the same $\{n\}$; our procedure ensures the possibility of defining the connected contribution of a configuration.

We may introduce the diagrammatic representation of oriented configurations, by drawing each oriented link (n_+, n_-) as a bundle of n links, of which n_+ bear a positively oriented arrow and n_- bear a negatively oriented arrow. Removing the arrows leaves us with a diagrammatic representation of (unoriented) configurations. One may easily become convinced that the algebraic notion of disconnection turns out to coincide with the geometrical one. In this representation, a disconnection is a set of subdiagrams such that their superposition reproduces the original diagram. An example of disconnection is drawn in Fig. 1.

Without belaboring this topic, which is widely discussed in the literature [13,14], we only recall that the connected part of a collection of n (abstract) objects is recursively defined by the condition that the set of n objects coincides with the sum of the connected parts of all its partitions, including the collection itself. In the presence of multiple copies of the same object, in standard perturbation theory a combinatorial factor appears, which is hidden in the character expansion; as a consequence, when subtracting disconnections one must take care of dividing by the corresponding symmetry factors in order to restore the correct normalization.

The definitions imply that the geometric features $\mathcal{S}$ and $\{L\}$ of all assignments belonging to a given configuration are the same; therefore the path p of a configuration is characterized by L_p and by the value n_p of the order of r_p.

C. Skeleton diagrams

It is convenient to reduce each configuration to its *skeleton diagram*, whose links are the paths of the configuration. The topology $\mathcal{S}$ is obviously unchanged, and each link is characterized by the pair of numbers (n_p, L_p).

In order to clarify the relevance of such a definition, let us consider the problem of evaluating the group integrals $R^{(\mathcal{S})}_{\{r,L\}}$ for the assignments belonging to a given configuration.
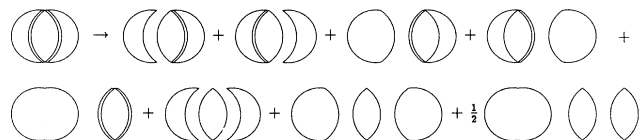
An elementary consequence of Eq. (4) is the evaluation

of the simplest nontrivial group integral entering our calculations:

$$\int dU \chi_{(r)}(A^\dagger U) \chi_{(r)}(U^\dagger B) = \frac{1}{d_{(r)}} \chi_{(r)}(A^\dagger B). \quad (23)$$

By applying repeatedly Eq. (23) along the paths we easily obtain

$$R^{(\mathcal{S})}_{\{r,L\}} = \left\{ \prod_{p=1}^{\nu} \left[\tilde{z}_{(r_p)} \right]^{L_p} \right\} S^{(\mathcal{S})}_{\{r\}}, \quad (24)$$

where ν the number of paths of the configuration, and $S^{(\mathcal{S})}_{\{r\}}$ is the value of the group integral associated with the skeleton diagram, in which all links are assigned unit length and weight, and representations are chosen according to the assignment. Further simplification is obtained by noticing that the effective strong-coupling variable in the character expansion is $z(\beta)$ [for large N actually $z(\beta) \approx \beta$ because of Eq. (12)]. Therefore by replacing the character coefficients $\tilde{z}_{(r)}$ with the ratios

$$z_{(r)} = \frac{\tilde{z}_{(r)}}{z^n}, \quad (25)$$

we may express the strong-coupling series as a series in powers of z, with coefficients that are functions of $z_{(r)}$; by the way, these quantities for large enough N are pure numbers, dependent on N but independent of β, because of Eq. (18). We can rewrite Eq. (24) as

$$R^{(\mathcal{S})}_{\{r,L\}} = z^{\sum_p n_p L_p} \left\{ \prod_{p=1}^{\nu} z_{(r_p)}^{L_p} \right\} S^{(\mathcal{S})}_{\{r\}}; \quad (26)$$

since $z_{1;0} \equiv 1$, there is no dependence on the lengths of the links with $n = 1$, apart from the overall factor of z, depending only on the total length of the configuration, $L = \sum_p n_p L_p$. Therefore the corresponding L_p indices can be dropped, thus defining a *reduced skeleton*. The contribution of a configuration to the functional integral is simply the sum of the contributions of all its assignments. It then follows from Eq. (26) that whenever two configurations can be reduced to the same skeleton, they will give the same contribution.

An exchange in the ordering of the vertices will not change the topology of a skeleton diagram; therefore configurations that are related by this symmetry will give the same contribution. Moreover, configurations sharing the same reduced skeleton will give contributions differing only by an overall proportionality factor, depending on the total length L. We can group together all configurations with the same reduced skeleton (taking into account the above-mentioned symmetry) and the same value of L: Their number is what we call the *geometrical factor*. The common value of each of these configurations is proportional to the *group-theoretical factor* of the reduced skeleton:

$$T^{(\mathcal{S})}_{\{n,L\}} = \sum_{\substack{\{r\} \\ \{n\}\ \text{fixed}}} \prod_{p=1}^{\nu} \left[z_{(r_p)} \right]^{L_p} S^{(\mathcal{S})}_{\{r\}}, \quad (27)$$

with a proportionality factor z^L.

The strong-coupling character expansion of a group integral can therefore be organized as a series in powers of

FIG. 1. All the nontrivial disconnections of a diagram.

$z \equiv \tilde{z}_{1;0}$, with coefficients obtained by taking the sums of products of geometrical and group-theoretical factors. In order to understand the computational simplifications achieved at this stage, let us only notice that, at different orders in the expansion, the same reduced skeletons may appear again and again in association with different values of L; their group-theoretical factors, however, are computed once and for all, while extracting the geometrical factors is a task that, as we shall show later, can be completely automatized.

D. Superskeletons

Both for the purpose of bookkeeping and in view of the problem of actually computing the group-theoretical factors, at this stage we need a classification and labeling of (reduced) skeleton diagrams, which must keep track of their topological properties and try to put into evidence whatever further simplification we may conceive. We found it convenient to isolate for each topology $\mathcal{S}$ a "core" topology $\mathcal{T}$ which we call a *superskeleton*, defined by the condition that each vertex in it is connected by at most a single link to any other vertex (i.e., the entries in the connectivity matrix are either 0 or 1).

The essential ingredient for the reduction of a skeleton to a superskeleton is the extraction of *bubbles*, defined as sets of two links in a skeleton connecting the same pair of vertices. Let us now recall the decomposition rule for a product of characters:

$$\chi_{(r)}(U)\,\chi_{(s)}(U) = \sum_t C_{(rst)}\,\chi_{(t)}(U)\,, \qquad (28)$$

where $C_{(rst)}$ is a set of integer numbers counting the multiplicity of (t) in the product of representations $(r) \otimes (s)$. For all assignments of (r), (s) consistent with a given skeleton, (t) must be such that the triplet (r), (s), $(\bar{t})$ satisfies Eqs. (21) and (22). Therefore replacing a bubble with a single link and allowing for all $\chi_{(t)}$ obtained from Eq. (28) to be inserted in it defines new consistent assignments. Notice, however, that in general we may not expect all these assignments to belong to the same skeleton, since n may vary within the class of admissible (t).

We can repeat the procedure, replacing paths with links when needed, consistently with orthogonality of representations and Eq. (23), until all the bubbles in the
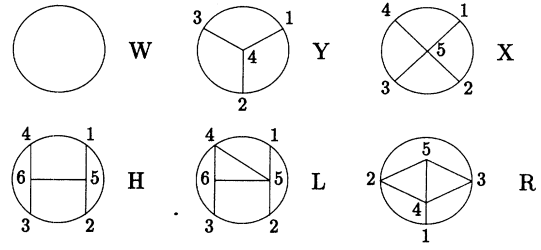

FIG. 2. Superskeleton topologies.

skeleton have disappeared. The resulting diagram is the superskeleton of our original diagram. We must stress that a superskeleton is *not* a skeleton diagram, because it does not make sense to assign a value of (n, L) to its links. It is, however, important to observe that the value $S^{(\mathcal{S})}_{\{r\}}$ of the group integral corresponding to any assignment $\{r\}$ on the skeleton $\mathcal{S}$ can be expressed as a weighted sum of factors $S^{(\mathcal{T})}_{\{t\}}$ corresponding to the consistent assignments of the superskeleton $\mathcal{T}$, with weights that are related to the factors

$$C_{(rst)}\,\frac{d_{(r)}d_{(s)}}{d_{(t)}} \qquad (29)$$

obtained by replacing bubbles with single links.

A superskeleton is completely identified by its topology, and it is worth mentioning that, as in the case of skeletons, superskeletons differing only by a permutation of vertices are equivalent, and therefore they can be reduced to a standard form. The number of different superskeletons that are relevant to a given order of the strong-coupling expansion is bound to grow with the order; however, for sufficiently low orders their number is so small that we found it convenient to label superskeletons by capital letters, in many cases related to their actual shapes. A provisional list of labelings is provided by Fig. 2.

This is the starting point of our classification scheme for skeletons. Reduced skeletons are named by the symbol denoting the topology of their superskeleton; the full information concerning superskeleton links, denoted by σ, will appear as arguments; using the pair of integers ij to denote the link connecting node i to node j, with node numbering fixed by Fig. 2, the skeletons will be named

$$W(\sigma)\,,$$
$$X(\sigma_{12}; \sigma_{23}; \sigma_{34}; \sigma_{41}; \sigma_{15}; \sigma_{25}; \sigma_{35}; \sigma_{45})\,,$$
$$L(\sigma_{12}; \sigma_{23}; \sigma_{34}; \sigma_{41}; \sigma_{36}; \sigma_{46}; \sigma_{15}; \sigma_{25}; \sigma_{56}; \sigma_{45})\,,$$

$$Y(\sigma_{12}; \sigma_{23}; \sigma_{31}; \sigma_{14}; \sigma_{24}; \sigma_{34})\,,$$
$$H(\sigma_{12}; \sigma_{23}; \sigma_{34}; \sigma_{41}; \sigma_{15}; \sigma_{25}; \sigma_{36}; \sigma_{46}; \sigma_{56})\,,$$
$$R(\sigma_{12}; \sigma_{23}; \sigma_{31}; \sigma_{14}; \sigma_{24}; \sigma_{25}; \sigma_{35}; \sigma_{34}; \sigma_{45})\,.$$

σ contains information about n and, for $n \neq 1$, also about the length L in the original skeleton and the bubble content. For reasons to be clarified later, we need not consider bubbles along $n = 1$ lines.

In general, a bubble will be denoted by $[\sigma_1; \sigma_2]$, where σ_1 and σ_2 contain the information about the bubble links. In summary, a link information will take one of the forms

$$n, p + q, [n_1, L_1; n_2, L_2] \qquad n, p, [n_1, L_1; [n_2, L_2; n_3, L_3]]$$
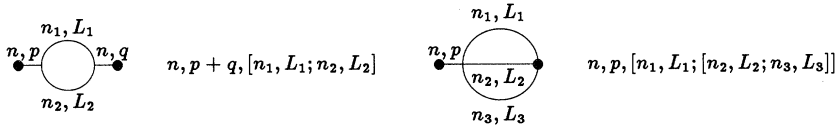
FIG. 3. Examples of bubbles.

$$\sigma = 1 \qquad (n = 1), \tag{30}$$

$$\sigma = n, L \qquad (n \neq 1, \text{ no bubble insertions}), \tag{31}$$

$$\sigma = n, L, [\sigma_{1,1}; \sigma_{1,2}][\sigma_{2,1}; \sigma_{2,2}], \ldots \qquad \text{(one or more bubble insertions on a line)}, \tag{32}$$

$$\sigma = [\sigma_{1,1}; \sigma_{1,2}][\sigma_{2,1}; \sigma_{2,2}], \ldots \qquad \text{(one or more bubble between two nodes)}, \tag{33}$$

the $\sigma_{i,j}$ themselves taking one of the above forms; insertion of b identical bubbles will be denoted by exponential notation, i.e., $[\sigma_1; \sigma_2]^b$. Examples of this notation are illustrated in Fig. 3.

E. Potentials

As we mentioned before, the possibility of defining the skeletons as sets of oriented configurations ensures the fact that we may consistently define the connected contribution of each skeleton diagram to the vacuum expectation value of an observable.

Since the geometrical notion of a disconnection only depends on the topology of a diagram, as a consequence of definitions we can define the (algebraic) connected contribution of a skeleton starting from its geometrical formulation. As a matter of fact, it is most convenient to exploit the fact that $n = 1$ lines cannot be split, and define the connected contribution of a reduced skeleton, i.e., the connected group-theoretical factor, which we shall call a *potential*:

$$P_{\{n,L\}}^{(\mathcal{S})} = \left[\sum_{\substack{\{r\} \\ \{n\} \text{ fixed}}} \prod_p \left[z_{(r_P)} \right]^{L_P} S_{\{r\}}^{(\mathcal{S})} \right]_{\text{connected}} \tag{34}$$

An example of the chain leading from an assignment to the superskeleton and to the potential is illustrated in Fig. 4.

When we are evaluating the skeletons contributing to the partition function, the sum of their potentials with the same geometrical factors is just the free energy. When computing the fundamental two-point function $G(x)$, no disconnection of the vacuum diagram can split the $n = 1$ line associated with the fundamental character $\mathrm{Tr}\, U^\dagger(x)\, U(0)$, and there is therefore a one-to-one correspondence between the connected contribution of a given skeleton diagram and the contribution of the associated vacuum diagram to the free energy. Moreover, the weight $d_{1;0}^{-2} = 1/N^2$ is the correct normalization, ensuring that in the large-N limit finite contributions to the Green's functions correspond to finite contributions to the free energy. From now on we may therefore focus on the evaluation of potentials related to vacuum skeleton diagrams.

When computing more general Green's functions, one must be careful not to include among the disconnections of the corresponding vacuum diagrams those splitting the line associated with the operator whose expectation value we are evaluating. Apart from this specification, the technique we have adopted to compute the fundamental Green's functions can be applied to the general case.

It is worth mentioning that we might have defined oriented potentials, but this notion, while conceptually useful, does not find any use in our actual computations.

A final observation concerns notation: We shall label potentials with the same symbols adopted in the labeling of the corresponding reduced skeletons.

We must draw some attention to the fact that our definition of potentials, although referred to unoriented diagrams, is originated by the problem of evaluating Green's functions. Therefore we are assuming that the orientation of one of the links has been fixed. By a trivial symmetry of conjugate representations, our potentials will be one-half of the corresponding vacuum contributions to the free energy.

Unlabeled links are (1;0)
Assignment   Oriented configuration   Configuration
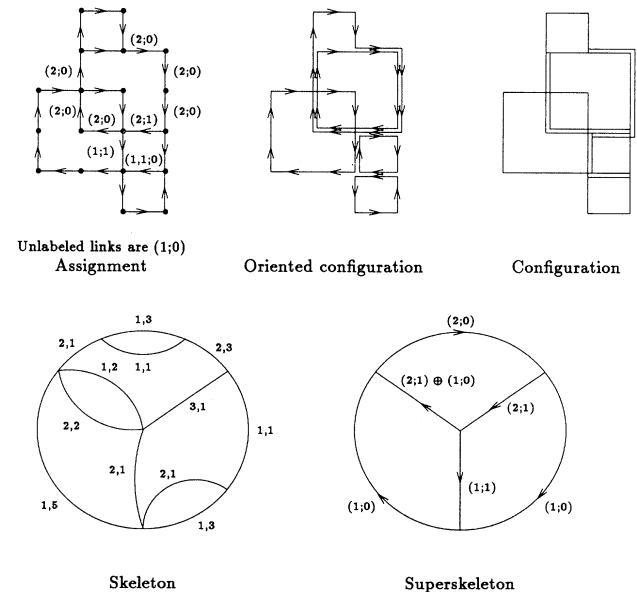
Skeleton   Superskeleton

FIG. 4. Steps showing that a sample assignment contributes to the potential $Y(1, [1; 2, 1]; 1; 2, 4, 1; 1; 1; [1; 2, 2]) = W(2, 1)\, Y(1; 1; 2, 4, 1; 1; 1; [1; 2, 2])$.

Including this factor of 2, the disconnections drawn in Fig. 1 can be written as

$$\mathrm{disc}\big(2W(2, L_1, [2, L_2; 2, 0, 1])\big)$$

$$\begin{aligned} &= 2 \times 2W(1) \times 2W(2, L_1, 1) + 2 \times 2W(1) \\ &\quad \times 2W(2, L_2, 1) + 2W(1) \times 2W(2, L_1+L_2) \\ &\quad + \tfrac{5}{2} \times [2W(1)]^3. \end{aligned} \tag{35}$$

IV. COMPUTING THE GEOMETRICAL FACTOR

The enumeration of all configurations possessing the same reduced skeleton can be completely automatized by the following considerations and procedures.

Equations (21) and (22) ensure the existence of a (non-necessarily unique) nonbacktracking random walk of length $\sum_p n_p L_p$ reproducing the diagrammatic representation of each configuration. We therefore generate all nonbacktracking random walks with fixed length, fixed origin 0, and fixed end x, and we compute the corresponding configurations $\{n\}$; i.e., we compute n_l (the number of times each link is visited) for each link of the lattice.

We now face the problem that the same configuration can be generated several times, from different paths. One approach we followed was to compare the generated configurations, and discard multiple copies, choosing one (and only one) walk for each different configuration. This approach suffers from the problem that every different configuration must be kept in the computer's random access memory (RAM) in order to do the comparison, and RAM becomes the limiting factor.

The total (bulk) free energy can be computed by summing over all the closed-loop configurations. Therefore the free energy *per site* can be computed by summing over all the configurations that are not related by a translation. These are easily obtained by generating all nonbacktracking closed random walks touching a given site, identifying the corresponding configurations, and choosing one configuration for each equivalence class under translation symmetry. From this point on, the computation is identical both for the Green's functions and for the free energy.

We must notice that at this point we have generated all the sets $\{n\}$ obeying Eqs. (21) and (22), but not all of them lead to nonvanishing group integrals; we get rid of these "null" configurations by defining their group-theoretical factor to be zero. Our computer program recognizes and automatically discards two classes of null diagrams.

(1) Diagrams that can be disconnected by removing a single node. A very simple property of invariant group integration allows for the possibility of setting a single integration variable to 1. As a consequence, one may prove that, whenever the removal of a vertex in a skeleton leaves us with disconnected subdiagrams, the value of the group integral factorizes into a product of terms that are just the values of its disconnected parts. Therefore, the

corresponding potentials vanish identically.

(2) Diagrams that can be disconnected by removing two links, unless the links share the same value of n. Such diagrams vanish as a trivial consequence of the orthogonality of representations.

Examples of these phenomena are drawn in Fig. 5.

We compute the reduced skeleton of each of these configurations. We now group together all the configurations which give origin to equivalent reduced skeletons (i.e., which are equal apart from a permutation of vertices); the geometrical factor is the number of such configurations.

To bypass the abovementioned RAM problem, we notice that the multiplicity of a configuration, i.e., the number of times it is generated by nonbacktracking random walks, depends only on its skeleton. Therefore we can skip the RAM-intensive step of comparing configurations, and just count the number of nonbacktracking random walks which generate the same skeleton. The geometrical factor is then obtained dividing this number by the multiplicity, which is the same for all the configurations contributing to the geometrical factor. The multiplicity is equal to the number of nonbacktracking random walks *on the skeleton* covering n_p times each link p, and therefore it can be computed by explicitly counting such walks. This approach completely solves the RAM problem, at a very small CPU time cost.

We factorize each skeleton "cutting" along $n = 1$ paths, identify bubbles according to the scheme of Sec. III D, and compute the connectivity of the corresponding superskeleton. The superskeleton is then either identified as in Fig. 2, or shown to originate from a null configuration. Finally we put together all this information to obtain the potential, and use the superskeleton symmetry to bring it to a standard form.

While the data needed in the intermediate stages of this computation can be extremely large, the results of the last step (potentials and geometrical factors) are rather compact and can be stored for further processing.

We computed all the Green's functions up to 18th order and the free energy up to 20th order on the square lattice (they of course involve several new superskeletons beside those drawn in Fig. 2). The longest computations took about 1 CPU hour on a HP-730/125.

At this stage we must clarify what we mean by a standard form of a superskeleton. In sufficiently complex cases, an ambiguity may arise as a consequence of different sequences of the elimination of the bubbles. While the resulting superskeleton is always the same, equivalent skeletons may receive superficially inequivalent labelings. We have not made an effort to reduce completely all these
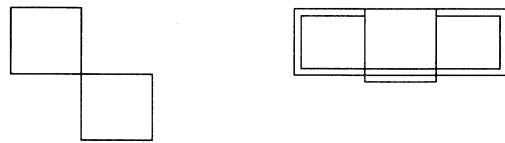

FIG. 5. Two null configurations: The first can be disconnected by removing a single node; the second can be disconnected by removing a $n = 1$ and a $n = 3$ link.

different namings to a standard form, but we were satisfied with the reduction to a common form in most cases. We checked explicitly that the computed values of differently labeled equivalent potentials are equal.

V. COMPUTING THE GROUP-THEORETICAL FACTOR

In contrast with the previous section, we must say that the evaluation of potentials is not yet fully automatized.

We can routinely generate all the sets $\{l; m\}$ needed to identify the representations of $U(N)$ to a definite order. The closed formulas presented in Sec. II enable us to evaluate automatically their dimensions and their large-N character coefficients.

We can perform the decomposition of the products of these representations, thus identifying the coefficients $C_{(rst)}$ and the factors defined in Eq. (29). We can therefore reduce the evaluation of the group-theoretical factors, by computer manipulations, to a linear combination with known coefficients of factors $S_{\{r\}}^{(\mathcal{T})}$, which are nothing but group integrals corresponding to consistent assignments of representations on the (unit length, unit weight) links of a superskeleton with topology $\mathcal{T}$.

Computing the factors $S_{\{r\}}^{(\mathcal{T})}$ is basically a sophisticated exercise in group integration, and it is therefore completely solved from a conceptual point of view. The group integration over a multiple product of representations can always be performed by decomposing the product into sums of representations, via the introduction of appropriate Clebsch-Gordan coefficients, and applying orthogonality of representations [Eq. (4)] in the last step. This may, however, become a very inconvenient procedure, essentially because of the fantastic proliferation of indices (all to be finally contracted, but appearing at intermediate stages already in the simplest examples) resulting from writing higher-order representations in the basis of polynomials of the fundamental representation.

We have not seriously tried to overcome this problem in general; i.e., we have no algorithm capable of generating the Clebsch-Gordan coefficients for the decomposition of the product of two arbitrary representations of $U(N)$, which would allow one to implement the relevant group integrations in a computer program. Instead we followed a slightly different approach, more limited in purpose and simpler to implement, within our self-imposed limits, without fully computerizing the computation.

The essentials of our approach are the following.

We observed that, for not very high orders of strong coupling, only a small number of superskeletons and low-order representations enter the calculation. Therefore, by

making use of a few well-known results of group integration (which can basically be derived from the knowledge of the six-matrix de Wit–'t Hooft integral [15]), we managed to compute explicitly all the factors $S_{\{r\}}^{(\mathcal{T})}$ entering in our calculations.

However, the possibility of inserting bubbles and varying the lengths L_s allows the generation of a huge number of different skeletons even starting from a very small set of assignments on a superskeleton. The group-theoretical factors of these skeletons can thus be evaluated symbolically on wide classes, as functions of the above parameters (which are the same entering the labeling of skeletons), and the explicit evaluation of the potentials entering an actual calculation can be implemented in a computer algebra program.

The procedure consisting in the generalization of each new object occurring at a definite order in the expansion to a whole family of more complicated objects and the symbolic evaluation of all the members of the family ensures a considerable reduction in the number of new objects appearing at each further step in the extension of the series.

A final comment concerns the opportunity of applying the above strategy directly to the computation of connected group-theoretical factors, i.e., of the potentials. The generation of disconnections can be performed algorithmically; however, in practice we found it simpler to resort to geometric arguments in the cases we analyzed explicitly. All these cases were simple enough for us to be able to write down compact symbolic expressions referring directly to the potentials. Some of our results will be presented in detail in the following sections.

VI. TECHNICAL REMARKS ON GROUP INTEGRATION

In evaluating quantities like $S_{\{r\}}^{(\mathcal{T})}$, one may take advantage of the invariance properties of the Haar measure for group integration:

$$d\mu(U) = d\mu(UA) = d\mu(AU), \tag{36}$$

in order to eliminate ("gauge") one of the variables (defined on the nodes of the diagram). A judicious use of gauging can induce notable simplifications in the actual computations, by replacing "open indices" (representations) with "closed indices" (characters) in the integrands, and decoupling many variables from each other.

As an illustrative example, let us consider the simplest nontrivial superskeleton. In principle we must evaluate

$$S_{r_1,r_2,r_3,r_4,r_5,r_6}^{(\mathrm{Y})} \propto \int \chi_{(r_1)}(AB^\dagger)\,\chi_{(r_2)}(BC^\dagger)\,\chi_{(r_3)}(CA^\dagger)\,\chi_{(r_4)}(A^\dagger D)\,\chi_{(r_5)}(B^\dagger D)\,\chi_{(r_6)}(C^\dagger D)\,dA\,dB\,dC\,dD\,. \tag{37}$$

However, by gauging the variable D we can reduce the previous expression to the factorized integral

$$S^{(Y)}_{r_1,r_2,r_3,r_4,r_5,r_6} \propto \int \chi_{(r_4)}(A^\dagger)\, \mathcal{D}^{\alpha\beta}_{(r_1)}(A)\, \mathcal{D}^{\mu\nu}_{(r_3)}(A^\dagger)\, dA$$

$$\times \int \chi_{(r_5)}(B^\dagger)\, \mathcal{D}^{\gamma\delta}_{(r_2)}(B)\, \mathcal{D}^{\beta\alpha}_{(r_1)}(B^\dagger)\, dB \int \chi_{(r_6)}(C^\dagger)\, \mathcal{D}^{\nu\mu}_{(r_3)}(C)\, \mathcal{D}^{\delta\gamma}_{(r_2)}(C^\dagger)\, dC, \tag{38}$$

whose factors in turn will be expressible in terms of the representations of the identity via the relationship

$$\int \chi_{(t)}(A^\dagger)\, \mathcal{D}^{\alpha\beta}_{(r)}(A)\, \mathcal{D}^{\gamma\delta}_{(s)}(A)\, dA = \sum_{(u)} \int \chi_{(t)}(A^\dagger)\, \mathcal{D}^{\mu\nu}_{(u)}(A)\, C_{(rsu)}{}^{\mu\nu}_{\alpha\beta\gamma\delta}\, dA$$

$$= \frac{1}{d_{(t)}}\, \delta^{\mu\nu}_{(t)} C_{(rst)}{}^{\mu\nu}_{\alpha\beta\gamma\delta} = \frac{1}{d_{(t)}}\, \delta^{(t)}_{\alpha\gamma,\beta\delta}, \tag{39}$$

where $C_{(rst)}{}^{\mu\nu}_{\alpha\beta\gamma\delta}$ are the Clebsch-Gordan coefficients and $\delta^{(t)}_{\alpha\gamma,\beta\delta}$ are the (not necessarily irreducible) representations of the identity.

We shall call these factors "gauged vertices," and present a few explicit examples, because they are essential ingredients of most of the actual computations we have performed; it is immediately apparent that proper gauging can reduce the evaluation of all X (as well as Y) superskeletons to contractions of gauged vertices.

The simplest nontrivial vertex involves two $n = 1$ representations and one $n = 2$ representation. There are three $n = 2$ representations, which we write down adopting the notation

$$\mathcal{D}^{ik,jl}_\pm(A) = \tfrac{1}{2}\left[A_{ij}A_{kl} \pm A_{il}A_{kj}\right], \tag{40}$$

$$\mathcal{D}^{ik,jl}_{1;1}(A) = A_{ij}A^\dagger_{lk} - \frac{1}{N}\,\delta_{ik}\delta_{jl}, \tag{41}$$

where $\mathcal{D}_+ = \mathcal{D}_{2;0}$ and $\mathcal{D}_- = \mathcal{D}_{1,1;0}$. One can easily show that the (ungauged) vertices are

$$\int \mathcal{D}^{ik,jl}_\pm(A)A^\dagger_{ab}A^\dagger_{cd} = \frac{1}{d_\pm}\,\delta^{(\pm)}_{ik,bd}\,\delta^{(\pm)}_{ac,jl}$$

$$= \frac{1}{4d_\pm}\left(\delta_{ib}\delta_{kd} \pm \delta_{id}\delta_{kb}\right)\left(\delta_{aj}\delta_{cl} \pm \delta_{al}\delta_{cj}\right), \tag{42}$$

$$\int \mathcal{D}^{ik,jl}_{1;1}(A)A_{ba}A^\dagger_{cd} = \frac{1}{d_{1;1}}\,\delta^{(1;1)}_{ik,db}\delta^{(1;1)}_{ca,jl}$$

$$= \frac{1}{d_{1;1}}\left(\delta_{id}\delta_{bk} - \frac{1}{N}\delta_{ik}\delta_{db}\right)\left(\delta_{cj}\delta_{al} - \frac{1}{N}\delta_{ca}\delta_{jl}\right). \tag{43}$$

The gauged vertices are trivially obtained by contraction of indices, and correspond to the representations of the identity matrix in the form (40), (41). Equations (42) and (43) may also be used in the evaluation of a few integrals belonging to superskeletons with topology H.

The next vertices in order of difficulty involve one each of the $n = 1$, $n = 2$, and $n = 3$ representations. Adopting for $n = 3$ representations the notation

$$\chi^{(3)}_+ = \chi_{3;0}, \qquad \chi^{(3)}_- = \chi_{1,1,1;0}, \qquad \chi^{(2,1)}_+ = \chi_{2;1}, \qquad \chi^{(2,1)}_- = \chi_{1,1;1}, \tag{44}$$

we may express the corresponding vertices in the form

$$\int \chi^{(3)}_\pm(A)\, \mathcal{D}^{ik,jl}_\pm(A^\dagger)\, A^\dagger_{mn}\, dA = \frac{1}{d^{(3)}_\pm}\, \delta^{(3)}_\pm(ikm, jln), \tag{45}$$

$$\int \chi_{2,1;0}(A)\, \mathcal{D}^{ik,jl}_\pm(A^\dagger)\, A^\dagger_{mn}\, dA = \frac{1}{d^{(1,2;0)}}\, \delta^{(1,2;0)}_\pm(ikm, jln), \tag{46}$$

$$\int \chi^{(2;1)}_\pm(A)\, \mathcal{D}^{ik,jl}_{1;1}(A)\, A^\dagger_{mn}\, dA = \frac{1}{d^{(2;1)}_\pm}\, \delta^{(2;1)}_\pm(ikn, jlm), \tag{47}$$

$$\int \chi^{(2;1)}_\pm(A)\, \mathcal{D}^{lm,kn}_\pm(A^\dagger)\, A_{ij}\, dA = \frac{1}{d^{(2;1)}_\pm}\, \delta^{(2;1)}_\pm(ikn, jlm), \tag{48}$$

where

$$\delta^{(3)}_\pm(ikm, jln) = \tfrac{1}{6}\left[\delta_{ij}\delta_{kl}\delta_{mn} + \delta_{il}\delta_{kn}\delta_{mj} + \delta_{in}\delta_{kj}\delta_{ml} \pm \delta_{il}\delta_{kj}\delta_{mn} \pm \delta_{ij}\delta_{kn}\delta_{ml} \pm \delta_{in}\delta_{kl}\delta_{mj}\right], \tag{49}$$

$$\delta^{(1,2;0)}_\pm(ikm, jln) = \tfrac{1}{6}\left[2\delta_{ij}\delta_{kl}\delta_{mn} - \delta_{il}\delta_{kn}\delta_{mj} - \delta_{in}\delta_{kj}\delta_{ml} \pm 2\delta_{il}\delta_{kj}\delta_{mn} \mp \delta_{ij}\delta_{kn}\delta_{ml} \mp \delta_{in}\delta_{kl}\delta_{mj}\right], \tag{50}$$

$$\delta^{(2;1)}_\pm(ikn, jlm) = \tfrac{1}{2}\left[\delta_{ij}\delta_{kl}\delta_{nm} \pm \delta_{ij}\delta_{km}\delta_{nl}\right] - \frac{1}{2(N \pm 1)}\left[\delta_{ik}\delta_{jl}\delta_{nm} \pm \delta_{ik}\delta_{jm}\delta_{nl} \pm \delta_{in}\delta_{jl}\delta_{km} + \delta_{in}\delta_{jm}\delta_{kl}\right]. \tag{51}$$

Aside from a few technicalities, the results from group integration presented in this section are essentially all that is needed for an evaluation of the full 15th-order strong-coupling contribution to the fundamental two-point Green's functions of the two-dimensional chiral model on the square lattice.

VII. COMPUTING THE POTENTIALS

The quantities that we have denoted with the general symbol $P_{\{n,L\}}^{(S)}$ and called *potentials* are the connected parts of sums over the sets of representations consistent with the geometry of a given skeleton diagram. Needless to say, knowledge of compact analytic expressions for wide classes of potentials can only dramatically simplify the task of evaluating explicitly high orders of the character expansion. In turn, since the reduction of any diagram to its superskeleton can be performed algorithmically, simplifying the problem of diagram recognition, it would be obviously pleasant to possess expressions for potentials general enough to be applied to superskeletons instead of individual skeletons.

We made some progress in this direction, classifying all and evaluating most of the skeleton diagrams whose superskeletons are drawn in Fig. 2 and obey the constraint $n \leq 3$ for all links. In this section we shall present some general considerations and all the results that are needed for an explicit evaluation of all $G(x)$ up to 12th order. We computed many more potentials, but often results are too cumbersome to make their presentation useful in any sense; they are available upon request from the authors.

We recall that the potentials are labeled by the same symbols attributed to the corresponding skeleton diagrams.

We already mentioned that the length of the $n = 1$ links does not enter the definition of the potentials. Moreover, the bubble content of the $n = 1$ links is factorized; i.e., the connected value of the full diagram is simply the product of the connected values of the diagram without bubble insertion and the diagram obtained by closing the bubble on itself and dividing by N^2; both these quantities are just lower-order potentials. The proof of factorization is very simple, and can be obtained immediately by gauging one of the vertices of the bubble and integrating over the second vertex variable.

This explains why we decided not to have a notation for skeletons with bubbles along $n = 1$ paths: Their name and value are expressed by the product of their factors.

Let us now consider bubble insertions on nontrivial links $n \neq 1$, in order of difficulty. The simplest case involves insertion of a bubble formed by two $n = 1$ lines between two vertices. Let us work out this example in detail in order to explain the general procedure. We take the product of representations

$$\big((1;0) \oplus (0;1)\big) \otimes \big((1;0) \oplus (0;1)\big)$$

$$= (2;0) \oplus (1,1;0) \oplus (0;2) \oplus (0;1,1) \oplus (1;1)$$
$$\oplus (1;1) \oplus (0;0) \oplus (0;0). \qquad (52)$$

We must recognize that the existence of such a bubble implies the possibility of two disconnections of the total diagram, corresponding of the two orientations of the closed path running around the bubble. Therefore the connected contribution of the bubble is obtained by removing the two $(0;0)$ representations from the product, and amounts simply to replacing the bubble with a single $n = 2$ line (of length $L = 0$), with weight obtained from Eq. (29) and expressible in the form

$$B_\pm \equiv \frac{N^2}{d_\pm} \quad \text{for } \mathcal{D}_\pm \,, \qquad B_{1;1} \equiv \frac{2N^2}{d_{1;1}} \quad \text{for } \mathcal{D}_{1;1} \,. \quad (53)$$

Given the ubiquitous presence of insertions of such bubbles along $n = 2$ lines, we will adopt the shorthand notation

$$\sigma = 2, L, b, \dots \equiv 2, L, [1;1]^b, \dots \qquad (54)$$

for the insertion of b $[1;1]$ bubbles. Such insertions imply the replacements

$$d_\pm \to d_\pm (B_\pm)^b, \qquad (55)$$
$$d_{1;1} \to d_{1;1}(B_{1;1})^b, \qquad (56)$$

in the expression for the value of the corresponding superskeleton, and the inclusion of a factor 2^b in front of all the disconnections corresponding to a splitting of the $n = 2$ line.

We may now consider the insertion of a bubble $[1;2]$ between two vertices. According to the rules for the product of representations, the corresponding contribution is obtained by replacing the bubble either with an $n = 1$ line or with an $n = 3$ line (with different weights attached to different $n = 3$ representations). In the first case we may apply the previously discussed factorization, while in the second case it is convenient to define the *bubble factors* $B(a, b)$ as

$$d_\pm^{(3)} B_\pm^{(3)}(a, b) = N d_\pm z_\pm^a B_\pm^b, \qquad (57)$$
$$d_{2,1;0} B_{2,1;0}(a, b) = N d_+ z_+^a B_+^b + N d_- z_-^a B_-^b, \qquad (58)$$
$$d_\pm^{(2,1)} B_\pm^{(2,1)}(a, b) = N d_\pm z_\pm^a B_\pm^b + N d_{1;1} z_{1;1}^a B_{1;1}^b. \qquad (59)$$

The insertion of the set of k bubbles $[2, a_1, b_1; 1] \cdots [2, a_k, b_k; 1]$ along an $n = 3$ line can now be accounted for by the following substitutions in the expression of the superskeleton:

$$d_\pm^{(3)} \to d_\pm^{(3)} \prod_{i=1}^{k} B_\pm^{(3)}(a_i, b_i), \qquad (60)$$

$$d_{2,1;0} \to d_{2,1;0} \prod_{i=1}^{k} B_{2,1;0}(a_i, b_i), \qquad (61)$$

$$d_\pm^{(2,1)} \to d_\pm^{(2,1)} \prod_{i=1}^{k} B^{(2,1)}(a_i, b_i). \qquad (62)$$

Moreover, one must introduce factors of 2^{b_i} in the disconnections involving the splitting of the ith $n = 2$ line, and a factor 3^k in the disconnections involving the full splitting of the $n = 3$ line into $n = 1$ lines.

Next in order of difficulty are the rules concerning the insertions of [1, 3] and [2; 2] bubbles. In each case the allowed replacements involve either an $n = 2$ or an $n = 4$ line.

The bubble factors to be inserted along an $n = 4$ line are essentially trivial generalizations of our previous examples whose expressions we shall not exhibit explicitly.

The $n = 2$ case is more interesting, because it is the first instance of a new phenomenon: the occurrence of disconnections of the skeleton diagram not corresponding

to disconnections of the superskeleton. As one may easily understand, these disconnections correspond to lower-order bubbles that may be removed from the skeleton turning it into another acceptable skeleton. This possibility can be systematically taken into account by defining *connected* bubble insertions.

Let us therefore introduce the bubble factors $B(p; a_1, b_1; ...; a_r, b_r)$, corresponding to the insertion of $[1; 3, p, [1; 2, a_1, b_1] \cdots [1; 2, a_r, b_r]]$, and $C(a_1, b_1; a_2, b_2)$, corresponding to the insertion of $[2, a_1, b_1; 2, a_2, b_2]$:

$$d_{\pm} B_{\pm}(p; a_1, b_1; ...; a_r, b_r) = N d_{\pm}^{(3)} \left(z_{\pm}^{(3)}\right)^p \prod_{i=1}^{r} B_{\pm}^{(3)}(a_i, b_i) + N d_{2,1;0} z_{2,1;0}^p \prod_{i=1}^{r} B_{2,1;0}(a_i, b_i)$$

$$+ N d_{\pm}^{(2,1)} \left(z_{\pm}^{(2,1)}\right)^p \prod_{i=1}^{r} B_{\pm}^{(2,1)}(a_i, b_i) - 2N^2 d_{\pm} z_{\pm}^p \prod_{i=1}^{r} \left(z_{\pm}^{a_i} B_{\pm}^{b_i} + 2^{b_i} B_{\pm}\right), \tag{63}$$

$$d_{1;1} B_{1;1}(p; a_1, b_1; ...; a_r, b_r) = N d_{+}^{(2,1)} \left(z_{+}^{(2,1)}\right)^p \prod_{i=1}^{r} B_{+}^{(2,1)}(a_i, b_i) + N d_{-}^{(2,1)} \left(z_{-}^{(2,1)}\right)^p \prod_{i=1}^{r} B_{-}^{(2,1)}(a_i, b_i)$$

$$- N^2 d_{1;1} z_{1;1}^p \prod_{i=1}^{r} \left(z_{1;1}^{a_i} B_{1;1}^{b_i} + 2^{b_i} B_{1;1}\right), \tag{64}$$

$$d_{\pm} C_{\pm}(a_1, b_1; a_2, b_2) = d_{1;1} z_{1;1}^{a_1} B_{1;1}^{b_1} \left[d_{+} z_{+}^{a_2} B_{+}^{b_2} + d_{-} z_{-}^{a_2} B_{-}^{b_2}\right] + d_{1;1} z_{1;1}^{a_2} B_{1;1}^{b_2} \left[d_{+} z_{+}^{a_1} B_{+}^{b_1} + d_{-} z_{-}^{a_1} B_{-}^{b_1}\right] - 2N^4 2^{b_1 + b_2}, \tag{65}$$

$$d_{1;1} C_{1;1}(a_1, b_1; a_2, b_2) = d_{1;1}^2 z_{1;1}^{a_1 + a_2} B_{1;1}^{b_1 + b_2} + \left[d_{+} z_{+}^{a_1} B_{+}^{b_1} + d_{-} z_{-}^{a_1} B_{-}^{b_1}\right] \left[d_{+} z_{+}^{a_2} B_{+}^{b_2} + d_{-} z_{-}^{a_2} B_{-}^{b_2}\right] - 2N^4 2^{b_1 + b_2}. \tag{66}$$

When considering disconnections of these diagrams, one must be careful to include only those that have a corresponding term among the disconnections of the super-skeleton.

These rules are the essential ingredients for the construction of the connected contributions of all the skeleton diagrams entering our 15th-order calculations. In particular, all potentials entering 12th-order calculations can be obtained by the above-mentioned insertions into the superskeletons drawn in Fig. 6.

The values of these potentials are reported in Appendix A. Here we will only report the results concerning

$W(2, ...)$, for reference and illustration of our formalism.

We first recall that $W(1)$ is completely trivial: $W(1) = 1$ and the associated geometrical factor is related to the number of self-avoiding random walks of length equal to the power of z.

For the most general potential related to $W(2, L)$ we are interested in, the main $n = 2$ line splits into q [1; 1] bubbles, r [2; 2] bubbles (the bubble links themselves splitting into $b_{i,1}$ and $b_{i,2}$ [1; 1] bubbles), and s [3; 1] bubbles (the $n = 3$ link splitting into u_j [2; 1] bubbles, each $n = 2$ link splitting into b'_{jk} [1; 1] bubbles). We obtained the value of the potentials in the form

$$N^2 W(2, L, q, [2, a_{1,1}, b_{1,1}; 2, a_{1,2}, b_{1,2}] \cdots [2, a_{r,1}, b_{r,1}; 2, a_{r,2}, b_{r,2}]$$
$$\times [1; 3, p_1, [2, a'_{1,1}, b'_{1,1}; 1] \cdots [2, a'_{1,u_1}, b'_{1,u_1}; 1]] \cdots [1; 3, p_s, [2, a'_{s,1}, b'_{s,1}; 1] \cdots [2, a'_{s,u_s}, b'_{s,u_s}; 1]])$$

$$= z_{+}^L d_{+}^2 B_{+}^q \prod_{j=1}^{s} B_{+}(p_j, a'_{j,1}, b'_{j,1}, ..., a'_{j,u_j}, b'_{j,u_j}) \prod_{i=1}^{r} C_{+}(a_{i,1}, b_{i,1}, a_{i,2}, b_{i,2})$$

$$+ z_{-}^L d_{-}^2 B_{-}^q \prod_{j=1}^{s} B_{-}(p_j, a'_{j,1}, b'_{j,1}, ..., a'_{j,u_j}, b'_{j,u_j}) \prod_{i=1}^{r} C_{-}(a_{i,1}, b_{i,1}, a_{i,2}, b_{i,2})$$

$$+ \frac{1}{2} z_{1;1}^L d_{1;1}^2 B_{1;1}^q \prod_{j=1}^{s} B_{1;1}(p_j, a'_{j,1}, b'_{j,1}, ..., a'_{j,u_j}, b'_{j,u_j}) \prod_{i=1}^{r} C_{1;1}(a_{i,1}, b_{i,1}, a_{i,2}, b_{i,2})$$

$$- 2^{q+r+s} N^4 \prod_{j=1}^{s} \sum_{\mathcal{P}(u_j)} 2^{\sum_{m \notin \mathcal{P}(u_j)} b'_{j,m}} W \left(2, p_j + \sum_{k \in \mathcal{P}(u_j)} a'_{j,k}, u_j + \sum_{k \in \mathcal{P}(u_j)} (b'_{j,k} - 1)\right)$$

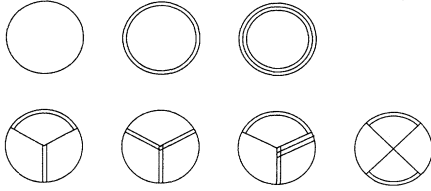$$\times \prod_{i=1}^{r} [2^{b_{i,2}} W(2; a_{i,1}, b_{i,1}) + 2^{b_{i,1}} W(2; a_{i,2}, b_{i,2})], \tag{67}$$

FIG. 6. Superskeletons corresponding to potentials appearing up to 12th order.

where $\mathcal{P}(u_j)$ are all the subsets of $\{1, ..., u_j\}$, and $\sum_{m \notin \mathcal{P}(u_j)}$ is a shorthand for $\sum_{m \in \{1,...,u_j\} \backslash \mathcal{P}(u_j)}$.

VIII. TWO-POINT GREEN'S FUNCTIONS AND THE INVERSE PROPAGATOR

The techniques and results presented in the previous sections set the stage for the evaluation of the strong-coupling series for the two-point Green's functions $G(x)$ of $U(N) \times U(N)$ principal chiral models on a two-dimensional square lattice, as functions of x, $z(\beta)$, and of the potentials. At any finite order q of the strong-coupling expansion, only a finite number of coordinate space Green's functions are nonzero, owing to the fact that the leading contribution comes from the shortest walk connecting x with the origin, which is proportional to $z^{|x_1|+|x_2|}$; therefore all Green's functions such that $|x_1| + |x_2| > q$ vanish. The number of nontrivial Green's functions, exploiting discrete symmetries, is, therefore,

$$\tfrac{1}{4}(q + 2)^2 \quad (q \text{ even}), \qquad \tfrac{1}{4}(q + 1)(q + 3) \quad (q \text{ odd}). \quad (68)$$

Coordinate space Green's functions are the natural output of a strong-coupling computation. Listing their individual strong-coupling series is, however, by no means the most compact and physically most appealing way of presenting the results. It is certainly convenient to introduce the lattice momentum transform

$$\tilde{G}(p) = \sum_x G(x) \exp(ip \cdot x), \qquad (69)$$

which, because of the lattice symmetries, turns out to be a function of the symmetric combinations of $\cos n_1 p_1$ and $\cos n_2 p_2$, with $n_1, n_2 \leq q$.

A really dramatic simplification, however, occurs only when we take into consideration the inverse lattice propagator $\tilde{G}^{-1}(p)$. Indeed, because of the recursive nature of the path-generating process, any strong-coupling expansion admitting a reinterpretation as a summation over paths can be seen, at any definite order in the expansion, as originating from a generalized Gaussian model in which the appearance of new structures violating lower-order recursion equations can be seen as the effect of quasilocal interactions that appear in the inverse propagator as Fourier transforms of non-nearest-neighbor couplings. A new structure capable of violating the recursion must correspond to a nontrivial path topology, with the property of multiply connecting the end points. Such a path must necessarily be at least three times as long as the minimal path. This argument shows that, in contrast with Eq. (69), in the inverse propagator combinations of $\cos n_1 p_1$ and $\cos n_2 p_2$ may appear only for $n_1, n_2 \leq q/3$. A more refined analysis shows that the highest values of n_1 and n_2 generated in $\tilde{G}^{-1}(p)$ to order q in the expansion are

$$n_1, n_2 \leq u - 2 \quad (q = 3u - 2), \qquad n_1, n_2 \leq u - 1 \quad (q = 3u - 1),$$
$$n_1, n_2 \leq u \quad (q = 3u) \qquad (u \text{ integer}). \qquad (70)$$

A more immediate physical interpretation of the results is obtained by introducing the traditional function

$$\hat{p}_\mu = 2 \sin \frac{p_\mu}{2} \qquad (71)$$

and expressing $\tilde{G}^{-1}(p)$ as a function of $\hat{p}_\mu^2 = 2(1 - \cos p_\mu)$. One may easily get convinced that the number of independent symmetric combinations of powers of $\hat{p}_\mu^2$ entering a given order in the expansion of $\tilde{G}^{-1}(p)$ is equal to the number of independent effective couplings one might define at the same order, consistently with the above-mentioned considerations. This is in turn related to the number of lattice sites, not related by a lattice symmetry transformation, such that $|x_1| + |x_2| \leq u$. We found that

a natural basis for the parametrization of these independent combinations is offered by

$$\hat{p}^{2s} \big[(\hat{p}^2)^2 - \hat{p}^4\big]^t, \qquad s + 2t \leq u, \qquad (72)$$

where

$$\hat{p}^0 = 1, \qquad \hat{p}^{2s} = \sum_\mu \hat{p}_\mu^{2s} \quad (s \geq 1). \qquad (73)$$

We also found that terms with $t \neq 0$ appear in $\tilde{G}^{-1}(p)$ at order $q = 3(s + 2t)$, while terms with $t = 0$ appear only at order $q = 3s + 2$; the implication of this phenomenon will be discussed later.

We will therefore make use of the parametrization

$$\tilde{G}^{-1}(p) = A_0 + A_1 \hat{p}^2 + \sum_{u=2}^{\infty} \sum_{\substack{s=0 \\ u-s \text{ even}}}^{u} A_{u,s} \hat{p}^{2s} \big[(\hat{p}^2)^2 - \hat{p}^4\big]^{(u-s)/2} \qquad (74)$$

to present our strong-coupling results for the inverse propagator in the form of expansions for the coefficients $A_{u,s}$. As already mentioned, the expansions of $A_{u,s}$ will be power series on z, starting with z^{3u} when $s \neq u$ and with z^{3u+2}

when $s = u$, with coefficients that are polynomials in the potentials.

The large-N limit of the $A_{u,s}$ is

$$
\begin{aligned}
A_0 = 1 &- 4\,z + 4\,z^2 - 4\,z^3 + 12\,z^4 - 28\,z^5 + 52\,z^6 - 132\,z^7 + 324\,z^8 - 908\,z^9 + 2020\,z^{10} \\
&- 6284\,z^{11} + 15\,284\,z^{12} - 48\,940\,z^{13} + 116\,612\,z^{14} - 393\,132\,z^{15} + O(z^{16}),
\end{aligned}
\tag{75a}
$$

$$
\begin{aligned}
A_1 = z &+ z^3 + 7\,z^5 + 4\,z^6 + 33\,z^7 + 32\,z^8 + 243\,z^9 + 324\,z^{10} + 1819\,z^{11} + 2520\,z^{12} \\
&+ 14\,859\,z^{13} + 23\,084\,z^{14} + 123\,883\,z^{15} + O(z^{16}),
\end{aligned}
\tag{75b}
$$

$$
A_{2,0} = -z^6 - 6\,z^8 - 8\,z^9 - 57\,z^{10} - 116\,z^{11} - 500\,z^{12} - 1152\,z^{13} - 5155\,z^{14} - 11\,632\,z^{15} + O(z^{16}),
\tag{75c}
$$

$$
A_{2,2} = -2\,z^8 - 4\,z^9 - 24\,z^{10} - 70\,z^{11} - 242\,z^{12} - 816\,z^{13} - 2824\,z^{14} - 8528\,z^{15} + O(z^{16}),
\tag{75d}
$$

$$
A_{3,1} = z^9 + \tfrac{29}{2}\,z^{11} + 26\,z^{12} + 144\,z^{13} + 482\,z^{14} + 1806\,z^{15} + O(z^{16}),
\tag{75e}
$$

$$
A_{3,3} = 2\,z^{11} + 4\,z^{12} + 40\,z^{13} + 140\,z^{14} + 548\,z^{15} + O(z^{16}),
\tag{75f}
$$

$$
A_{4,0} = -\tfrac{5}{2}\,z^{12} - 37\,z^{14} - 84\,z^{15} + O(z^{16}),
\tag{75g}
$$

$$
A_{4,2} = -z^{12} - 31\,z^{14} - 64\,z^{15} + O(z^{16}),
\tag{75h}
$$

$$
A_{4,4} = -2\,z^{14} - 4\,z^{15} + O(z^{16}),
\tag{75i}
$$

$$
A_{5,1} = 7\,z^{15} + O(z^{16}),
\tag{75j}
$$

$$
A_{5,3} = z^{15} + O(z^{16}).
\tag{75k}
$$

We have computed all $A_{u,s}$ to $O(z^{15})$ as functions of the potentials, but the results will not be presented here, for reasons explained in the Introduction. We shall limit ourselves to the presentation in Appendix C of 15th-order expressions as explicit functions of z and N. These functions are obtained by substituting Eq. (10) for the character expansion coefficients, obtaining the values of the potentials as N-dependent coefficients, and summing up all homogeneous contributions.

The limitations of such a procedure can easily be identified: qth-order expressions are correct for $U(N)$ groups with $N \geq q/2$ and for $SU(N)$ groups with $N \geq q + 2$. Even symbolic expressions for potentials suffer from some limitations, essentially because for small N not all the representations formally introduced are really nontrivial or independent. A manifestation of this fact is the appearance of the so-called 't Hooft–De Wit poles, which plague $U(N)$ strong-coupling expressions when $N \leq (q-2)/4$. In $SU(N)$ another limitation comes from the occurrence of self-dual representations, which spoil

the applicability of $U(N)$ results already for $N \leq q/2$.

In practice the results we have presented hold as they stand for all $U(N)$ groups with $N > 7$, while by using 12th-order expressions in terms of potentials one might obtain with a minor effort 15th-order expressions correct for all $N > 3$. $SU(N)$ groups are correctly reproduced for $N > 16$, and by use of 8th-order potentials one might obtain all $N > 7$.

We must, however, stress that in their most abstract formulation, i.e., when expressed as weighted combinations of connected group-theoretical factors, our results are fully general and apply not only to principal chiral models but also to many nonlinear σ models on group manifolds admitting a character expansion, including $O(N)$ models.

A number of physically interesting quantities can be extracted from $\tilde{G}^{-1}(p)$ by appropriate manipulations. In the present section we will only present the large-N limit of some of them. In particular we obtain the magnetic susceptibility

$$
\begin{aligned}
\chi = \sum_x G(x) = \frac{1}{A_0} = 1 &+ 4\,z + 12\,z^2 + 36\,z^3 + 100\,z^4 + 284\,z^5 + 796\,z^6 + 2276\,z^7 + 6444\,z^8 + 18\,572\,z^9 \\
&+ 53\,292\,z^{10} + 155\,500\,z^{11} + 451\,516\,z^{12} + 1\,330\,796\,z^{13} + 3\,904\,908\,z^{14} + 11\,617\,356\,z^{15} + O(z^{16}).
\end{aligned}
\tag{76}
$$

By defining the second moment of the correlation functions

$$
\chi\langle x^2 \rangle_G = \frac{1}{4}\sum_x x^2 G(x) = \frac{A_1}{A_0^2},
\tag{77}
$$

we can introduce the second-moment definition of the correlation length

$$
\begin{aligned}
M_G^2 = \frac{1}{\langle x^2 \rangle_G} = \frac{A_0}{A_1} = \frac{1}{z} &- 4 + 3\,z + 2\,z^3 - 4\,z^4 + 12\,z^5 - 40\,z^6 + 84\,z^7 - 296\,z^8 + 550\,z^9 - 1904\,z^{10} \\
&+ 3316\,z^{11} - 15\,248\,z^{12} + 27\,756\,z^{13} + O(z^{14})
\end{aligned}
\tag{78}
$$

and the corresponding wave function renormalization

$$Z_G = \frac{1}{A_1} = z + z^3 + 7\,z^5 + 4\,z^6 + 33\,z^7 + 32\,z^8 + 243\,z^9 + 324\,z^{10}$$
$$+ 1819\,z^{11} + 2520\,z^{12} + 14\,859\,z^{13} + 23\,084\,z^{14} + 123\,883\,z^{15} + O\!\left(z^{16}\right). \tag{79}$$

The true mass gap should in principle be extracted from the long-distance behavior of the two-point Green's function:

$$\mu = -\lim_{|x|\to\infty} \ln \frac{G(x)}{|x|} . \tag{80}$$

This quantity is, however, related by standard analyticity properties to the imaginary momentum pole singularity of $\tilde{G}(p)$, and we can therefore extract the mass gap by solving the equation

$$\tilde{G}^{-1}(p_1{=}i\mu_s, p_2{=}0) = 0. \tag{81}$$

In absence of strict rotation invariance, this quantity is to be interpreted as the wall-wall correlation length. Let us notice that Eq. (81) involves only the coefficients $A_{u,u}$ in the expansion (74) of $\tilde{G}^{-1}(p)$. The power series of these coefficients in turn start with z^{3u+2} and are associated with factors $\hat{p}^{2u}$. Equation (81) is therefore, order

by order in the strong-coupling expansion, algebraic and series expandable in the variable

$$zM_s^2 = 2z(\cosh\mu_s - 1). \tag{82}$$

By recalling the properties of $A_{u,u}$ one can easily get convinced that knowledge of $\tilde{G}^{-1}(p)$ to $O(z^{3u-1})$ and $O(z^{3u})$ allows for the determination of μ_s to $O(z^{2u})$ and $O(z^{2u+1})$, respectively. There is a deep connection between the orders of the strong-coupling expansion "lost" in the evaluation of μ_s and the above-mentioned considerations of the appearance of structures violating the recursive relationships among paths. Indeed these structures break down the exponentiation of the wall-wall correlation functions at short distances [16,17,2], and one is easily convinced that loss of exponentiation at a distance $\sim u$ implies from Eq. (80) a residual precision $\sim 2u$ in the determination of μ.

The resulting value is

$$\mu_s = -\ln z - 2\,z - \tfrac{2}{3}\,z^3 - 2\,z^4 - \tfrac{42}{5}\,z^5 - 8\,z^6 - \tfrac{310}{7}\,z^7 - 70\,z^8 - \tfrac{3188}{9}\,z^9 - 520\,z^{10} - \tfrac{28778}{11}\,z^{11} - \tfrac{13154}{3}\,z^{12} + O\!\left(z^{13}\right). \tag{83}$$

In full analogy with the discussion above, we may consider the equation for the diagonal mass gap (i.e., the diagonal wall-wall correlation length):

$$\tilde{G}^{-1}(p_1{=}i\mu_d/\sqrt{2}, p_2{=}i\mu_d/\sqrt{2}) = 0. \tag{84}$$

Equation (84) is algebraic and series expandable in

$$zM_d^2 = 4z\left(\cosh\frac{\mu_d}{\sqrt{2}} - 1\right). \tag{85}$$

Moreover, one may show that zM_d^2 is an even function of z, and knowledge of $\tilde{G}^{-1}(p)$ to $O(z^{3u})$ allows for the determination of μ_d to $O(z^{2u})$. The result is

$$\mu_d = -\ln 2z - z^2 - 3\,z^4 - \tfrac{119}{6}\,z^6 - 136\,z^8 - \tfrac{41963}{40}\,z^{10} + O\!\left(z^{12}\right). \tag{86}$$

Our results for the side and diagonal mass gap in terms of potentials, up to $O(z^{12})$ and $O(z^{11})$, respectively, are available as explained in the Introduction. They are presented in form of explicit functions of N and z in Appendix C. In order to compute the 12th-order contribution to μ_s, we evaluated a few long-distance Green's functions to $O(z^{16})$ and $O(z^{17})$.

The analytic properties of the strong-coupling series (radius of convergence, zeroes of partition function, critical behavior) are best studied by considering such bulk quantities as the free energy

$$F(\beta) = \frac{1}{N^2 V} \ln \int \prod_x dU(x) \exp(-S_L), \tag{87}$$

the internal energy

$$E(\beta) = 1 - \frac{1}{4}\frac{\partial F}{\partial \beta} = 1 - G((1,0)), \tag{88}$$

and the specific heat

$$C(\beta) = -\beta^2 \frac{\partial E}{\partial \beta} = \frac{1}{4}\beta^2 \frac{\partial^2 F}{\partial \beta^2}. \tag{89}$$

We were able to generate 20th-order series for the free energy per site F in terms of the potentials introduced in Fig. 6; the results are available as explained in the Introduction. We shall only present here the explicit expression for large N up to 18th order, and report the result in terms of N and β in Appendix C, with the usual warning that they hold only for U(N), $N \geq 9$ and SU(N), $N > 18$:

$$F = 2z^2 + 2z^4 + 4z^6 + 19z^8 + 96z^{10} + 604z^{12} + 4036z^{14} + \frac{58471}{2}z^{16} + \frac{663184}{3}z^{18} + O(z^{20}). \qquad (90)$$

For large but finite N, we can use Eq. (12) to replace the derivative with respect to β in Eq. (88) with a derivative with respect to z, thus obtaining a relationship between F and $G((1,0))$, which we verified explicitly. It should be noticed that no simple relationship between F and $G((1,0))$ can be obtained in terms of potentials.

IX. STRONG-COUPLING EXPANSION ON THE HONEYCOMB LATTICE

On the honeycomb lattice we consider the action with nearest-neighbor interaction, which can be written as a sum over all links of the lattice:

$$S_h = -2N\beta \sum_{\text{links}} \text{Re} \, \text{Tr} \, [U_l U_r^\dagger], \qquad (91)$$

where l, r indicate the sites at the ends of each link. As on the square lattice, the link length a is chosen as the lattice spacing, i.e., as the length unit. The continuum action of chiral models is obtained from the $a \to 0$ limit of S_h by identifying

$$T = \frac{\sqrt{3}}{N\beta}. \qquad (92)$$

For what concerns the strong-coupling expansion, we only mention that the determination of the geometrical factor is straightforward in the light of our general discussion. The only difference with the square lattice concerns the generation of nonbacktracking random walks. It is easy to see that the honeycomb lattice can be mapped in a subset of the square lattice, having the same sites, the same links in the y direction, and only the links in the x directions starting from even sites: Therefore the walks on the honeycomb lattice are a subset of the walks on the square lattice. The value of the potentials is obviously unchanged, but since the computation can be pushed some orders further on the honeycomb lattice a few new calculations are needed. The only subtle point is that, since only half of the sites of the lattice are related by translation invariance, the free energy per site is one-half of the quantity computed according to Sec. IV.

We generated strong-coupling series of the free energy up to $O(z^{26})$ and of the fundamental Green's function up to $O(z^{20})$. Our results as functions of the potentials are available as explained in the Introduction. We present here only the large-N results; we refer to Appendix E for results for large but finite N.

In analogy with the square lattice, we evaluated the strong-coupling series of the fundamental correlation function $G(x) = \frac{1}{N} \langle \text{Tr} \, [U(x)U^\dagger(0)] \rangle$ as a function of x, $z(\beta)$ and of the potentials. The number of nontrivial components of $G(x)$ which must be evaluated at a given order q is

$$\frac{q^2 + 3q + 4}{4} \quad \text{if} \quad q = 4k, 4k+1 \,,$$

$$\frac{q^2 + 3q + 2}{4} \quad \text{if} \quad q = 4k+2, 4k+3 \,, \qquad (93)$$

with k an integer.

The magnetic susceptibility χ and second-moment correlation length ξ_G are defined on the honeycomb lattice in perfect analogy with square-lattice definitions:

$$\chi = \sum_x G(x), \quad \chi \xi_G^2 = \tfrac{1}{4} \sum_x x^2 G(x).$$

The analysis of models on honeycomb lattices presents some complications, which will be illustrated in some detail in Appendix E by considering a simple Gaussian model of random walks. The point is that, unlike square and triangular lattices, not all sites are related by a translation; this fact does not allow a straightforward definition of a Fourier transform. Only sites at an even distance (in the number of links) are related by a translation. We therefore define even and odd fields U_e, U_o: $U_e(x) = U(x)$ for even x, zero for odd x, and $U_o(x) = U(x)$ for odd x, zero for even x (the parity is defined with respect to an arbitrarily chosen origin). We then define the even and odd correlation functions:

$$G_e(x - y) = \frac{1}{N} \langle \text{Tr} \, [U_e(x)U_e^\dagger(y)] \rangle$$

$$= \frac{1}{N} \langle \text{Tr} \, [U_o(x)U_o^\dagger(y)] \rangle \,,$$

$$G_o(x - y) = \frac{1}{N} \langle \text{Tr} \, [U_e(x)U_o^\dagger(y)] \rangle$$

$$= \frac{1}{N} \langle \text{Tr} \, [U_o(x)U_e^\dagger(y)] \rangle \,. \qquad (94)$$

Since even and odd sites lie on two distinct triangular sublattices, it is possible to define consistent Fourier transforms on each sublattice.

Guided by the analysis of the Gaussian model, we considered two orthogonal wall-wall correlation functions:

$$G_1^{(w)}(x) = \sum_y G_e(x, y), \qquad (95)$$

$$G_2^{(w)}(x) = \sum_y [G_e(x, y) + G_o(x, y)]. \qquad (96)$$

In the strong-coupling domain both $G_1^{(w)}(x)$ and $G_2^{(w)}(x)$ enjoy exponentiation for a sufficiently large lattice distance, allowing the definition of the two corresponding masses μ_1 and μ_2:

$$G_1^{(w)}(x) \propto \exp\left(-\tfrac{3}{2}\mu_1 x\right), \qquad (97)$$

$$G_2^{(w)}(x) \propto \exp\left(-\tfrac{1}{2}\sqrt{3}\mu_2 x\right). \qquad (98)$$

In the continuum limit $\mu_1 = \mu_2$ and they both should reproduce the physical mass M propagating in the fundamental channel. The ratio μ_1/μ_2 allows a test of rota-

tional invariance, in analogy with the side/diagonal mass ratio of the square lattice. It is also possible to define the quantities

$$zM_1^2 = \tfrac{8}{9}z\left(\cosh\tfrac{3}{2}\mu_1 - 1\right), \qquad (99)$$

$$zM_2^2 = \tfrac{8}{3}z\left(\cosh\tfrac{1}{2}\sqrt{3}\mu_2 - 1\right), \qquad (100)$$

which play the role of zM_s^2 and zM_d^2 in the determination of the imaginary momentum pole of the inverse Fourier-transformed Green's function.

In full analogy with the square lattice, we define the magnetic susceptibility

$$\chi = \sum_x G(x) = 1 + 3\,z + 6\,z^2 + 12\,z^3 + 24\,z^4 + 48\,z^5 + 90\,z^6 + 174\,z^7 + 348\,z^8 + 702\,z^9$$
$$+ 1392\,z^{10} + 2814\,z^{11} + 5658\,z^{12} + 11\,532\,z^{13} + 23\,706\,z^{14} + 49\,368\,z^{15} + 101\,436\,z^{16}$$
$$+ 211\,290\,z^{17} + 440\,598\,z^{18} + 928\,614\,z^{19} + 1\,950\,390\,z^{20} + O\left(z^{21}\right), \qquad (101)$$

the second moment of the correlation functions

$$\chi\left\langle x^2\right\rangle_G = \frac{1}{4}\sum_x\left\{(9x_1^2 + 3x_2^2)G_e(x) + [(3x_1 - 1)^2 + 3x_2^2]G_o(x)\right\}, \qquad (102)$$

and the second-moment definition of the correlation length

$$M_G^2 = \frac{1}{\langle x^2\rangle_G} = \tfrac{4}{3}\,z^{-1} - 4 + \tfrac{8}{3}\,z - 8\,z^6 + \tfrac{40}{3}\,z^7 + 8\,z^8 - 16\,z^9 - 88\,z^{10} + 96\,z^{11}$$
$$- 144\,z^{12} + \tfrac{584}{3}\,z^{13} - 40\,z^{14} - 200\,z^{15} - 5520\,z^{16} + 5848\,z^{17} - 4208\,z^{18} + O\left(z^{19}\right). \qquad (103)$$

We were able to obtain 26th-order results in terms of potentials for the free energy per site:

$$F = \tfrac{3}{2}\,z^2 + z^6 + 3\,z^{10} + 9\,z^{12} + 12\,z^{14} + 114\,z^{16} + \tfrac{829}{3}\,z^{18} + 1080\,z^{20} + 5754\,z^{22}$$
$$+ \tfrac{34015}{2}\,z^{24} + 87\,396\,z^{26} + O\left(z^{28}\right). \qquad (104)$$

The internal energy (per link) and the specific heat can be obtained by

$$E(\beta) = 1 - \frac{1}{3}\frac{\partial F(\beta)}{\partial\beta} = 1 - G((1,0)), \qquad (105)$$

$$C(\beta) = -\beta^2\frac{\partial E}{\partial\beta} = \frac{1}{3}\beta^2\frac{\partial^2 F(\beta)}{\partial\beta^2}. \qquad (106)$$

The same caveats of the square-lattice case apply to the relationship between F and $G((1,0))$.

APPENDIX A: VALUES OF SELECTED POTENTIALS

In Sec. VII we reported a rather general form for potentials related to $W(2, L)$ by bubble insertions. Here

we present all potentials needed for a 12th-order computation and some generalizations. We also list all other potentials we computed; their expressions are too long and cumbersome to be reported here, and they are available upon request from the authors.

Let us introduce a shorthand notation for bubble insertion. A sequence of r $[1; 2]$ bubbles will be denoted by

$$\mathcal{I}_r(a_1, b_1, ..., a_r, b_r) \equiv [1; 2, a_1, b_1]\cdots[1; 2, a_r, b_r]; \qquad (A1)$$

the arguments $(a_1, b_1, ..., a_r, b_r)$ will often be left understood. A sequence of r $[2; 2]$ bubbles and s $[1; 3]$ bubbles (with $[1; 2]$ splittings along the $n = 3$ line) will be denoted by

$$\mathcal{I}_{r,s}(a_{1,1}, b_{1,1}, a_{2,1}, b_{2,1}, ..., a_{1,r}, b_{1,r}, a_{2,r}, b_{2,r}; p_1, a_1^1, b_1^1, ..., a_{u_1}^1, b_{u_1}^1; ...; p_s, a_1^s, b_1^s, ..., a_{u_s}^s, b_{u_s}^s)$$

$$\equiv [2, a_{1,1}, b_{1,1}; 2, a_{2,1}, b_{2,1}]\cdots[2, a_{1,r}, b_{1,r}; 2, a_{2,r}, b_{2,r}]$$
$$\times[1; 3, p_1, \mathcal{I}_{u_1}(a_1^1, b_1^1, ..., a_{u_1}^1, b_{u_1}^1)]\cdots[1; 3, p_s, \mathcal{I}_{u_s}(a_1^s, b_1^s, ..., a_{u_s}^s, b_{u_s}^s)]; \qquad (A2)$$

the arguments $(a_{1,1}, ..., b_{u_s}^s)$ will also be left understood.

The shorthand notation

$$\mathcal{Z}_{(r)}(p, q) \equiv z_{(r)}^p d_{(r)}^q \qquad (A3)$$

will also be used.

Potentials related to $W(3, L)$ are easily obtained from the identity

$$W(3, L, \mathcal{I}_r) = W(2, a_r, b_r, [1; 3, L, \mathcal{I}_{r-1}]). \tag{A4}$$

One must, however, compute explicitly the $r = 0$ case

$$W(3, L) = \frac{1}{N^2} \left[\mathcal{Z}_+^{(3)}(L, 2) + \mathcal{Z}_-^{(3)}(L, 2) + \mathcal{Z}_{2,1;0}(L, 2) + \mathcal{Z}_+^{(2;1)}(L, 2) + \mathcal{Z}_-^{(2;1)}(L, 2) \right] - 2N^2 W(2, L) - \frac{2}{3}N^4. \tag{A5}$$

We have also computed $W(4, L, \mathcal{I}_{r,s})$, whose structure is similar to $W(2, L, b, \mathcal{I}_{r,s})$ presented in Sec. VII. More generally, we must mention that a generating functional for $W(n, L)$ can easily be constructed by exploiting the general strong-coupling solution of the chiral chain problem [16,17,2]. It is easy to become convinced that

$$\frac{1}{2N^2} \ln \sum_n \sum_{(r)} \mathcal{Z}_{(r)}(L, 2) z^{nL} = \sum_n W(n, L) z^{nL}, \tag{A6}$$

where the sum on the left-hand side (LHS) is extended to all representations with the same value of n. In principle, generating functionals for potentials with bubble insertions can also be constructed.

Let us now consider the first nontrivial superskeleton Y:

$$Y(2, a_1, b_1; 1; 1; 1; 1; 2, a_2, b_2) = z_{1;1}^{a_1+a_2} B_{1;1}^{b_1+b_2} + \frac{1}{2} N^2 z_{1;1}^{a_1} B_{1;1}^{b_1-1} \left(z_+^{a_2} B_+^{b_2+1} + z_-^{a_2} B_-^{b_2+1} \right)$$

$$+ \frac{1}{2} N^2 z_{1;1}^{a_2} B_{1;1}^{b_2-1} \left(z_+^{a_1} B_+^{b_1+1} + z_-^{a_1} B_-^{b_1+1} \right) - 2N^2 2^{b_1+b_2}; \tag{A7}$$

this quantity was first introduced in Ref. [5] for the special choice $b_1 = b_2 = 0$, and it was termed $\widetilde{W}_{a_1, a_2}$. We have also computed more general objects of the form $Y(2, a_1, b_1, \mathcal{I}_{r_1,s_1}; 1; 1; 1; 1; 2, a_2, b_2, \mathcal{I}_{r_2,s_2})$.

$$Y(1; 1; 1; 2, a_1, b_1; 2, a_2, b_2; 2, a_3, b_3) = \mathcal{Z}_{1;1}(a_1 + a_2 + a_3, 1)(d_{1;1} - 1)B_{1;1}^{b_1+b_2+b_3}$$

$$+ \left(z_{1;1}^{a_1} B_{1;1}^{b_1} \left\{ \left[\mathcal{Z}_+(a_2, 1)B_+^{b_2} + \mathcal{Z}_-(a_2, 1)B_-^{b_2} \right] \left[\mathcal{Z}_+(a_3, 1)B_+^{b_3} + \mathcal{Z}_-(a_3, 1)B_-^{b_3} \right] \right. \right.$$

$$\left. - \left[\mathcal{Z}_+(a_2 + a_3, 1)B_+^{b_2+b_3} + \mathcal{Z}_-(a_2 + a_3, 1)B_-^{b_2+b_3} \right] \right\}$$

$$\left. - 2N^2 2^{b_2+b_3} W(2, a_1, b_1) \right) + \text{permutations of indices} - 4N^4 2^{b_1+b_2+b_3}; \tag{A8}$$

the case $b_1 = b_2 = b_3 = 0$ was termed W_{a_1, a_2, a_3} in Ref. [5].

$$Y(3, p; 2, a_1, b_1; 1; 2, a_2, b_2; 1; 1)$$

$$= N \left[\mathcal{Z}_+^{(3)}(p, 1) z_+^{a_1+a_2} B_+^{b_1+b_2} + \mathcal{Z}_-^{(3)}(p, 1) z_-^{a_1+a_2} B_-^{b_1+b_2} \right.$$

$$+ \frac{1}{4} \mathcal{Z}_{2,1;0}(p, 1) \left(z_+^{a_1+a_2} B_+^{b_1+b_2} + 3 z_+^{a_1} B_+^{b_1} z_-^{a_2} B_-^{b_2} + 3 z_+^{a_2} B_+^{b_2} z_-^{a_1} B_-^{b_1} + z_-^{a_1+a_2} B_-^{b_1+b_2} \right)$$

$$+ \mathcal{Z}_+^{(2;1)}(p, 1) \left(z_{1;1}^{a_1} B_{1;1}^{b_1} z_+^{a_2} B_+^{b_2} + z_{1;1}^{a_2} B_{1;1}^{b_2} z_+^{a_1} B_+^{b_1} + z_{1;1}^{a_1+a_2} B_{1;1}^{b_1+b_2} \right)$$

$$\left. + \mathcal{Z}_-^{(2;1)}(p, 1) \left(z_{1;1}^{a_1} B_{1;1}^{b_1} z_-^{a_2} B_-^{b_2} + z_{1;1}^{a_2} B_{1;1}^{b_2} z_-^{a_1} B_-^{b_1} + z_{1;1}^{a_1+a_2} B_{1;1}^{b_1+b_2} \right) \right]$$

$$- 2N^2 W(2, p + a_1, b_1) 2^{b_2} - 2N^2 W(2, p + a_2, b_2) 2^{b_1} - 2N^2 W(2, p, 0) 2^{b_1+b_2} - 4N^4 2^{b_1+b_2}. \tag{A9}$$

We also computed a few generalizations: $Y(3, p, \mathcal{I}_r; 2, a_1, b_1; 1; 2, a_2, b_2; 1; 1)$, $Y(3, p, \mathcal{I}_r; 2, a_1, b_1; 2, a_2, b_2; 1; 1; 2, a_3, b_3)$.

Finally, we computed, for a few special values of the indices, $Y(3, p_1; 2, a_1; 1; 2, a_2; 1; 3, p_2)$.

The second nontrivial superskeleton is X. We computed

$$X(2, a_1, b_1; 1; 2, a_2, b_2; 1; 1; 1; 1)$$

$$= \left[\mathcal{Z}_+(a_1, 1)B_+^{b_1} + \mathcal{Z}_-(a_1, 1)B_-^{b_1} + \mathcal{Z}_{1;1}(a_1, 1)B_{1;1}^{b_1} \right] \left[\mathcal{Z}_+(a_2, 1)B_+^{b_2} + \mathcal{Z}_-(a_2, 1)B_-^{b_2} + \mathcal{Z}_{1;1}(a_2, 1)B_{1;1}^{b_2} \right]$$

$$+ \frac{N^4}{16} d_{1;1} \left(\mathcal{Z}_+(a_1, -1)B_+^{b_1} + \mathcal{Z}_-(a_1, -1)B_-^{b_1} + \frac{4}{N^2} \mathcal{Z}_{1;1}(a_1, -1)B_{1;1}^{b_1} \right)$$

$$\times \left(\mathcal{Z}_+(a_2, -1)B_+^{b_2} + \mathcal{Z}_-(a_2, -1)B_-^{b_2} + \frac{4}{N^2} \mathcal{Z}_{1;1}(a_2, -1)B_{1;1}^{b_2} \right) + N^2 \mathcal{Z}_{1;1}(a_1 + a_2, -1)B_{1;1}^{b_1+b_2}(d_{1;1} + 4)$$

$$- 2N^2 \left[2^{b_1} W(2, a_2, b_2) + 2^{b_2} W(2, a_1, b_1) \right] - 2^{b_1+b_2}(4N^4 + 2N^2). \tag{A10}$$

APPENDIX B: LIST OF POTENTIALS

We list here all the potentials appearing for the first time at each order of the strong-coupling expansion; we identify potentials differing only for the values of L and for the number b of $[1;1]$ bubbles provided that $b > 0$ (i.e., we do not identify $b = 0$ with $b \neq 0$). In the following formulas, L will indicate a generic value, and multiple occurrences of L in the same expressions indicate any combinations of Ls (i.e., they can take different values).

5th order:

$$W(2, L, b). \tag{B1}$$

9th order:

$$W(3, L, [1; 2, L]), \ W(3, L, [1; 2, L, b]), \ Y(2, L; 1; 1; 1; 1; 2, L). \tag{B2}$$

10th order:

$$Y(2, L; 2, L; 1; 1; 2, L; 1). \tag{B3}$$

11th order:

$$W(2, L, [2, L; 2, L, b]), \ Y(3, L; 2, L; 1; 2, L; 1; 1), \ Y(2, L; 1; 1; 1; 1; 2, L, b). \tag{B4}$$

12th order:

$$W(2, L, b, [2, L; 2, L]), \ W(3, L, [1; 2, L]^2), \ Y(2, L; 2, L; 1; 1; 2, L, b; 1),$$
$$Y(2, L, b; 1; 1; 1; 2, L), \ X(2, L; 1; 2, L; 1; 1; 1; 1). \tag{B5}$$

13th order:

$$W(3, L, [1; 2, L, [1; 3, L]]), \ W(4, L, [1; 3, L]), \ W(4, L, [2, L; 2, L, b]), \ W(2, L, b, [2, L; 2, L, b]),$$
$$Y(3, L; 2, L; 1; 2, L, b; 1; 1), \ Y(3, L; 2, L; 2, L; 1; 1; 2, L), \ Y(2, L; 1; 1; 1; 1; [1; 3, L]),$$
$$Y(2, L, b; 1; 1; 1; 2, L, b), \ Y(2, L, b; 2, L; 1; 1; 2, L; 1), \ X(2, L; 1; 1; 1; 1; 2, L; 2, L),$$
$$H(2, L; 1; 2, L; 1; 1; 1; 1; 2, L). \tag{B6}$$

14th order:

$$W(3, L, [1; 2, L, b, [1; 3, L]]), \ W(4, L, [1; 3, L, [1; 2, L]]), \ W(2, L, [1; [1; 2, L]^2]),$$
$$W(2, L, [2, L, b; 2, L, b]), \ W(3, L, [1; 2, L] [1; 2, L, b]), \ Y(3, L; 3, L; 2, L; 1; 2, L; 1),$$
$$Y(3, L; 2, L, b; 1; 2, L; 1; 1), \ Y(2, L; 1; 1; 1; [1; 2, L]; 2, L), \ Y(2, L; 2, L; 1; 1; [1; 3, L]; 1),$$
$$Y(2, L; 2, L, b; 1; 1; 2, L; 1), \ Y(2, L, [1; 3, L]; 1; 1; 1; 2, L), \ X(1; 1; 1; 1; 2, L; 2, L; 2, L; 2, L; 2, L),$$
$$X(2, L; 1; 2, L; 1; 3, L; 1; 1; 1), \ X(2, L; 1; 2, L, b; 1; 1; 1; 1), \ X(2, L, b; 1; 1; 1; 1; 2, L; 2, L),$$
$$H(1; 2, L; 1; 2, L; 1; 1; 1; 2, L), \ H(2, L; 2, L; 1; 1; 2, L; 1; 2, L; 1),$$
$$R(1; 1; 2, L; 1; 1; 2, L; 1; 1). \tag{B7}$$

15th order:

$$W(3, L, [1; 2, L, [2, L; 2, L]]), \ W(3, L, [1; 2, L, [2, L; 2, L, b]]), \ W(3, L, [3, L; 2, L, b]),$$
$$W(3, L, [[1; 2, L]; 2, L]), \ W(4, L, [2, L, b; 2, L, b]), \ W(3, L, [1; 2, L]^3),$$
$$Y(3, L; 2, L; 1; [1; 3, L]; 1; 1), \ Y(3, L; 2, L; 1; 2, L; 1; 3, L), \ Y(3, L; 2, L; 2, L; 1; 1; 2, L, b),$$
$$Y(3, L; 2, L, b; 1; 2, L, b; 1; 1), \ Y(3, L; 2, L, b; 2, L; 1; 1; 2, L), \ Y(4, L; 3, L; 2, L; 2, L; 1; 1),$$
$$Y(2, L; 1; 1; 1; 1; [2, L; 2, L]), \ Y(2, L; 1; 1; 1; 1; 2, L, [1; 3, L]), \ Y(2, L; 2, L; 1; [1; 2, L]; 2, L; 1),$$
$$Y(2, L, b; 1; 1; 1; 1; [1; 3, L]), \ Y(2, L, b; 2, L; 1; 1; 2, L, b; 1), \ Y(3, L, [1; 2, L]; 2, L; 1; 2, L; 1; 1),$$
$$Y(2, L, [1; 3, L]; 2, L; 1; 1; 2, L; 1), \ X(1; 1; 1; 1; 2, L; 2, L; 2, L; 2, L, b),$$
$$X(3, L; 2, L; 1; 2, L; 1; 1; 1; 1), \ X(2, L; 1; 1; 1; 1; 1; 2, L; 2, L, b),$$
$$X(2, L; 1; 1; 1; 3, L; 1; 2, L; 2, L), \ X(2, L; 2, L; 1; 1; 1; 2, L; 1; 2, L),$$
$$H(3, L; 2, L; 1; 1; 2, L; 1; 1; 2, L; 1), \ H(2, L; 1; 2, L; 1; 1; 1; 1; 2, L, b),$$
$$H(2, L; 1; 2, L; 3, L; 1; 1; 1; 1; 2, L), \ H(2, L; 1; 2, L, b; 1; 1; 1; 1; 2, L),$$
$$H(2, L; 3, L; 2, L; 1; 1; 1; 1; 2, L), \ H(2, L; 2, L; 2, L; 1; 1; 2, L; 2, L; 1; 1),$$
$$L(1; 2, L; 1; 2, L; 1; 2, L; 1; 1; 1; 1), \ L(2, L; 1; 1; 1; 2, L; 1; 1; 1; 1; 1),$$
$$L(2, L; 1; 2, L; 1; 1; 2, L; 1; 1; 1; 1). \tag{B8}$$

APPENDIX C: SQUARE-LATTICE RESULTS FOR FINITE N

We list in the present appendix the values of the quantities defined in Sec. VIII without further comments. The definition of these quantities and the range of validity of the results presented here is discussed in Sec. VIII:

$$A_0 = 1 - 4z + 4z^2 - 4z^3 + 12z^4 - 28z^5 + 4z^6 \frac{-17 + 13N^2}{N^2 - 1}$$

$$+ 12z^7 \frac{-13 + 22N^2 - 11N^4}{\left(N^2 - 1\right)^2} + 4z^8 \frac{101 - 158N^2 + 81N^4}{\left(N^2 - 1\right)^2} + 4z^9 \frac{-243 + 358N^2 - 227N^4}{\left(N^2 - 1\right)^2}$$

$$+ 4z^{10} \frac{2444 - 6391N^2 + 7193N^4 - 3577N^6 + 505N^8}{\left(N^2 - 4\right)\left(N^2 - 1\right)^3}$$

$$+ 4z^{11}\left(-23\,568 + 89\,928N^2 - 154\,753N^4 + 145\,700N^6\right.$$
$$\left. - 74\,058N^8 + 17\,674N^{10} - 1571N^{12}\right)\frac{1}{\left(N^2 - 4\right)^2\left(N^2 - 1\right)^4}$$

$$+ 4z^{12}\left(59\,312 - 227\,352N^2 + 401\,499N^4 - 379\,396N^6\right.$$
$$\left. + 189\,036N^8 - 43\,842N^{10} + 3821N^{12}\right)\frac{1}{\left(N^2 - 4\right)^2\left(N^2 - 1\right)^4}$$

$$+ 4z^{13}\left(-145\,008 + 560\,056N^2 - 1\,018\,759N^4 + 986\,360N^6\right.$$
$$\left. - 519\,366N^8 + 128\,954N^{10} - 12\,235N^{12}\right)\frac{1}{\left(N^2 - 4\right)^2\left(N^2 - 1\right)^4}$$

$$+ 4z^{14}\left(3\,296\,016 - 16\,590\,056N^2 + 38\,621\,009N^4\right.$$
$$- 50\,952\,462N^6 + 40\,255\,375N^8 - 18\,791\,194N^{10} + 4\,822\,317N^{12}$$
$$\left. - 617\,438N^{14} + 29\,153N^{16}\right)\frac{1}{\left(N^2 - 9\right)\left(N^2 - 4\right)^2\left(N^2 - 1\right)^5}$$

$$+ 4z^{15}\left(-73\,339\,344 + 453\,776\,040N^2 - 1\,300\,249\,437N^4\right.$$
$$+ 2\,195\,554\,892N^6 - 2\,367\,482\,622N^8 + 1\,669\,383\,326N^{10} - 759\,240\,644N^{12}$$
$$\left. + 212\,701\,682N^{14} - 34\,650\,066N^{16} + 2\,929\,064N^{18} - 98\,283N^{20}\right)$$
$$\times \frac{1}{\left(N^2 - 9\right)^2\left(N^2 - 4\right)^2\left(N^2 - 1\right)^6} + O\!\left(z^{16}\right), \tag{C1}$$

$$A_1 = z + z^3 + 7z^5 + 4z^6 \frac{N^2 + 1}{N^2 - 1} + 3z^7 \frac{13 - 22N^2 + 11N^4}{\left(N^2 - 1\right)^2} + 8z^8 \frac{-5 - 2N^2 + 4N^4}{\left(N^2 - 1\right)^2} + z^9 \frac{251 - 294N^2 + 243N^4}{\left(N^2 - 1\right)^2}$$

$$+ 4z^{10} \frac{-284 - 13N^2 + 441N^4 - 369N^6 + 81N^8}{\left(N^2 - 4\right)\left(N^2 - 1\right)^3}$$

$$+ z^{11}\left(24\,208 - 76\,936N^2 + 129\,833N^4 - 134\,180N^6 + 76\,114N^8\right.$$
$$\left. - 19\,562N^{10} + 1819N^{12}\right)\frac{1}{\left(N^2 - 4\right)^2\left(N^2 - 1\right)^4}$$

$$+ 8z^{12} \frac{-3632 + 2616N^2 + 3565N^4 - 8734N^6 + 7962N^8 - 2821N^{10} + 315N^{12}}{\left(N^2 - 4\right)^2\left(N^2 - 1\right)^4}$$

$$+ z^{13}\left(148\,848 - 456\,760N^2 + 879\,351N^4 - 922\,184N^6\right.$$
$$\left. + 540\,230N^8 - 146\,906N^{10} + 14\,859N^{12}\right)\frac{1}{\left(N^2 - 4\right)^2\left(N^2 - 1\right)^4}$$

$$+ 4z^{14}\left(-422\,352 + 796\,520N^2 - 475\,949N^4 - 864\,192N^6\right.$$
$$\left. + 2\,055\,327N^8 - 1\,703\,150N^{10} + 634\,345N^{12} - 102\,496N^{14} + 5771N^{16}\right)\frac{1}{\left(N^2 - 9\right)\left(N^2 - 4\right)^2\left(N^2 - 1\right)^5}$$

$$+ z^{15}\left(75\,941\,712 - 403\,857\,000N^2 + 1\,114\,656\,565N^4\right.$$
$$- 1\,899\,839\,324N^6 + 2\,117\,909\,054N^8 - 1\,584\,540\,590N^{10} + 779\,561\,548N^{12}$$
$$\left. - 235\,498\,610N^{14} + 40\,734\,002N^{16} - 3\,591\,112N^{18} + 123\,883N^{20}\right)$$
$$\times \frac{1}{\left(N^2 - 9\right)^2\left(N^2 - 4\right)^2\left(N^2 - 1\right)^6} + O\!\left(z^{16}\right), \tag{C2}$$

$$A_{2,0} = -z^6 \frac{N^2+1}{N^2-1} + 2\,z^8 \frac{4+2\,N^2-3\,N^4}{\left(N^2-1\right)^2} - 4\,z^9 \frac{1+8\,N^2+2\,N^4}{\left(N^2-1\right)^2}$$

$$+ z^{10} \frac{212-25\,N^2-355\,N^4+255\,N^6-57\,N^8}{\left(N^2-4\right)\left(N^2-1\right)^3} + 4\,z^{11} \frac{-5-100\,N^2+137\,N^4-12\,N^6-29\,N^8}{\left(N^2-1\right)^4}$$

$$+ 2\,z^{12} \frac{2608-1944\,N^2+195\,N^4+1992\,N^6-4278\,N^8+2001\,N^{10}-250\,N^{12}}{\left(N^2-4\right)^2\left(N^2-1\right)^4}$$

$$+ 8\,z^{13} \frac{60+1485\,N^2-1735\,N^4+520\,N^6+396\,N^8-144\,N^{10}}{\left(N^2-4\right)\left(N^2-1\right)^4}$$

$$+ z^{14}\,(303\,120-666\,632\,N^2+1\,554\,257\,N^4-1\,748\,152\,N^6$$

$$+ 205\,601\,N^8+831\,342\,N^{10}-468\,499\,N^{12}+86\,566\,N^{14}-5155\,N^{16})\frac{1}{\left(N^2-9\right)\left(N^2-4\right)^2\left(N^2-1\right)^5}$$

$$+ 4\,z^{15}\,(-3984-68\,344\,N^2+247\,735\,N^4-387\,636\,N^6$$

$$+ 321\,005\,N^8-97\,944\,N^{10}-30\,420\,N^{12}+21\,362\,N^{14}-2908\,N^{16})\frac{1}{\left(N^2-4\right)^2\left(N^2-1\right)^6} + O\!\left(z^{16}\right), \quad \text{(C3)}$$

$$A_{2,2} = -2\,z^8 \frac{N^2+1}{N^2-1} - 2\,z^9 \frac{1+8\,N^2+2\,N^4}{\left(N^2-1\right)^2} + 2\,z^{10} \frac{-9-7\,N^2+9\,N^4-12\,N^6}{\left(N^2-1\right)^3}$$

$$+ 2\,z^{11} \frac{-5-112\,N^2+155\,N^4-12\,N^6-35\,N^8}{\left(N^2-1\right)^4} + 2\,z^{12} \frac{64+54\,N^2+100\,N^4-52\,N^6-121\,N^8}{\left(N^2-1\right)^4}$$

$$+ 4\,z^{13} \frac{60+1917\,N^2-1843\,N^4+640\,N^6+606\,N^8-204\,N^{10}}{\left(N^2-4\right)\left(N^2-1\right)^4}$$

$$+ 2\,z^{14}\,(-7392+8144\,N^2-55\,774\,N^4+92\,342\,N^6-35\,882\,N^8$$

$$- 16\,810\,N^{10}+10\,745\,N^{12}-1412\,N^{14})\frac{1}{\left(N^2-4\right)^2\left(N^2-1\right)^5}$$

$$+ 2\,z^{15}\,(-4336-96\,968\,N^2+298\,881\,N^4-461\,772\,N^6$$

$$+ 413\,767\,N^8-131\,684\,N^{10}-48\,836\,N^{12}+32\,296\,N^{14}-4264\,N^{16})\frac{1}{\left(N^2-4\right)^2\left(N^2-1\right)^6} + O\!\left(z^{16}\right),$$

$$\text{(C4)}$$

$$A_{3,1} = z^9 \frac{1+8\,N^2+2\,N^4}{2\left(N^2-1\right)^2} + z^{11} \frac{5+100\,N^2-137\,N^4+12\,N^6+29\,N^8}{2\left(N^2-1\right)^4} + 2\,z^{12} \frac{14\,N^2+93\,N^4+13\,N^6}{\left(N^2-1\right)^3}$$

$$+ z^{13} \frac{-60-1485\,N^2+1735\,N^4-520\,N^6-396\,N^8+144\,N^{10}}{\left(N^2-4\right)\left(N^2-1\right)^4}$$

$$+ 2\,z^{14} \frac{11-25\,N^2+1585\,N^4-2366\,N^6+714\,N^8+241\,N^{10}}{\left(N^2-1\right)^5}$$

$$+ z^{15}\,(4368+68\,152\,N^2-230\,047\,N^4+463\,796\,N^6-576\,029\,N^8$$

$$+ 309\,400\,N^{10}-21\,332\,N^{12}-20\,786\,N^{14}+3612\,N^{16})\frac{1}{2\left(N^2-4\right)^2\left(N^2-1\right)^6} + O\!\left(z^{16}\right), \quad \text{(C5)}$$

$$A_{3,3} = 2\,z^{11} \frac{2\,N^2+N^4}{\left(N^2-1\right)^2} + 4\,z^{12} \frac{2\,N^2+9\,N^4+N^6}{\left(N^2-1\right)^3} + 4\,z^{13} \frac{18\,N^2+5\,N^6+10\,N^8}{\left(N^2-1\right)^4}$$

$$+ 4\,z^{14} \frac{1+5\,N^2+223\,N^4-334\,N^6+106\,N^8+35\,N^{10}}{\left(N^2-1\right)^5}$$

$$+ 2\,z^{15} \frac{5+300\,N^2-255\,N^4+866\,N^6-1612\,N^8+455\,N^{10}+274\,N^{12}}{\left(N^2-1\right)^6} + O\!\left(z^{16}\right), \quad \text{(C6)}$$

$$A_{4,0} = -z^{12} \frac{4\,N^2 + 33\,N^4 + 5\,N^6}{2\left(N^2-1\right)^3} + z^{14} \frac{-2 + 10\,N^2 - 241\,N^4 + 362\,N^6 - 105\,N^8 - 37\,N^{10}}{\left(N^2-1\right)^5}$$

$$- 3\,z^{15} \frac{1 + 2\,N^2 + 39\,N^4 + 296\,N^6 + 28\,N^8}{\left(N^2-1\right)^4} + O\!\left(z^{16}\right), \tag{C7}$$

$$A_{4,2} = -z^{12} \frac{2\,N^2 + 9\,N^4 + N^6}{\left(N^2-1\right)^3} + z^{14} \frac{-1 - 5\,N^2 - 207\,N^4 + 306\,N^6 - 98\,N^8 - 31\,N^{10}}{\left(N^2-1\right)^5}$$

$$- 2\,z^{15} \frac{1 + 2\,N^2 + 69\,N^4 + 360\,N^6 + 32\,N^8}{\left(N^2-1\right)^4} + O\!\left(z^{16}\right), \tag{C8}$$

$$A_{4,4} = -2\,z^{14} \frac{4\,N^4 + N^6}{\left(N^2-1\right)^3} - 2\,z^{15} \frac{15\,N^4 + 32\,N^6 + 2\,N^8}{\left(N^2-1\right)^4} + O\!\left(z^{16}\right), \tag{C9}$$

$$A_{5,1} = z^{15} \frac{1 + 2\,N^2 + 39\,N^4 + 296\,N^6 + 28\,N^8}{4\left(N^2-1\right)^4} + O\!\left(z^{16}\right), \tag{C10}$$

$$A_{5,3} = z^{15} \frac{15\,N^4 + 32\,N^6 + 2\,N^8}{2\left(N^2-1\right)^4} + O\!\left(z^{16}\right), \tag{C11}$$

$$\mu_s = -\ln\left(z\right) - 2\,z - \tfrac{2}{3}z^3 - 2\,z^4 + 2\,z^5 \frac{1 - 21\,N^2}{5\left(N^2-1\right)} + 2\,z^6 \frac{-5 + 6\,N^2 - 4\,N^4}{\left(N^2-1\right)^2} + 2\,z^7 \frac{6 + 114\,N^2 - 155\,N^4}{7\left(N^2-1\right)^2}$$

$$+ 2\,z^8 \frac{22 - 64\,N^2 + 58\,N^4 - 35\,N^6}{\left(N^2-1\right)^3} + 2\,z^9 \frac{-104 - 1286\,N^2 + 9748\,N^4 - 15\,331\,N^6 + 8810\,N^8 - 1594\,N^{10}}{9\left(N^2-4\right)\left(N^2-1\right)^4}$$

$$+ 2\,z^{10} \frac{-1600 + 8768\,N^2 - 14\,596\,N^4 + 13\,482\,N^6 - 8645\,N^8 + 2500\,N^{10} - 260\,N^{12}}{\left(N^2-4\right)^2\left(N^2-1\right)^4}$$

$$+ 2\,z^{11} \left(-864 - 20\,592\,N^2 + 266\,170\,N^4 - 740\,050\,N^6\right.$$

$$\left. + 869\,302\,N^8 - 508\,486\,N^{10} + 141\,781\,N^{12} - 14\,389\,N^{14}\right) \frac{1}{11\left(N^2-4\right)^2\left(N^2-1\right)^5}$$

$$+ 2\,z^{12} \left(-23\,392 + 184\,400\,N^2 - 571\,030\,N^4 + 920\,690\,N^6\right.$$

$$\left. - 927\,373\,N^8 + 643\,901\,N^{10} - 289\,681\,N^{12} + 68\,171\,N^{14} - 6577\,N^{16}\right) \frac{1}{3\left(N^2-4\right)^2\left(N^2-1\right)^6} + O\!\left(z^{13}\right), \tag{C12}$$

$$\mu_d = -\ln\left(2z\right) - z^2 + z^4 \frac{2 - 3\,N^2}{N^2-1} + z^6 \frac{-79 + 248\,N^2 - 238\,N^4}{12\left(N^2-1\right)^2}$$

$$+ z^8 \frac{908 - 5299\,N^2 + 12\,080\,N^4 - 13\,391\,N^6 + 6844\,N^8 - 1088\,N^{10}}{8\left(N^2-4\right)\left(N^2-1\right)^4}$$

$$+ z^{10} \left(172\,816 - 1\,265\,528\,N^2 + 3\,877\,481\,N^4 - 6\,436\,255\,N^6\right.$$

$$\left. + 6\,193\,060\,N^8 - 3\,331\,306\,N^{10} + 864\,838\,N^{12} - 83\,926\,N^{14}\right) \frac{1}{80\left(N^2-4\right)^2\left(N^2-1\right)^5} + O\!\left(z^{12}\right), \tag{C13}$$

$$\chi = 1 + 4z + 12z^2 + 36z^3 + 100z^4 + 284z^5 + 4z^6 \frac{-195 + 199N^2}{N^2 - 1} + 4z^7 \frac{543 - 1106N^2 + 569N^4}{(N^2 - 1)^2}$$

$$+ 12z^8 \frac{493 - 1022N^2 + 537N^4}{(N^2 - 1)^2} + 4z^9 \frac{4067 - 8550N^2 + 4643N^4}{(N^2 - 1)^2}$$

$$+ 4z^{10} \frac{44\,100 - 149\,869N^2 + 182\,355N^4 - 90\,083N^6 + 13\,323N^8}{(N^2 - 4)(N^2 - 1)^3}$$

$$+ 4z^{11} (481\,168 - 2\,256\,648N^2 + 4\,239\,673N^4 - 4\,010\,564N^6$$
$$+ 1\,961\,034N^8 - 452\,890N^{10} + 38\,875N^{12}) \frac{1}{(N^2 - 4)^2 (N^2 - 1)^4}$$

$$+ 4z^{12} (1\,299\,728 - 6\,161\,736N^2 + 11\,712\,625N^4$$
$$- 11\,228\,076N^6 + 5\,568\,300N^8 - 1\,301\,614N^{10} + 112\,879N^{12}) \frac{1}{(N^2 - 4)^2 (N^2 - 1)^4}$$

$$+ 4z^{13} (3\,526\,000 - 16\,894\,776N^2 + 32\,535\,287N^4$$
$$- 31\,650\,616N^6 + 15\,957\,638N^8 - 3\,784\,938N^{10} + 332\,699N^{12}) \frac{1}{(N^2 - 4)^2 (N^2 - 1)^4}$$

$$+ 4z^{14} (85\,479\,984 - 509\,240\,632N^2 + 1\,277\,936\,387N^4$$
$$- 1\,742\,114\,314N^6 + 1\,385\,750\,301N^8 - 641\,889\,782N^{10} + 163\,736\,431N^{12}$$
$$- 20\,707\,322N^{14} + 976\,227N^{16}) \frac{1}{(N^2 - 9)(N^2 - 4)^2 (N^2 - 1)^5}$$

$$+ 4z^{15} (2\,078\,977\,104 - 14\,813\,458\,920N^2 + 45\,842\,748\,421N^4$$
$$- 80\,400\,814\,700N^6 + 87\,447\,748\,126N^8 - 60\,663\,055\,822N^{10} + 26\,640\,570\,340N^{12}$$
$$- 7\,157\,578\,626N^{14} + 1\,112\,718\,466N^{16} - 90\,043\,336N^{18} + 2\,904\,339N^{20})$$
$$\times \frac{1}{(N^2 - 9)^2 (N^2 - 4)^2 (N^2 - 1)^6} + O(z^{16}), \tag{C14}$$

$$M_G^2 = z^{-1} - 4 + 3z + 2z^3 - 4z^4 \frac{N^2 + 1}{N^2 - 1} + 2z^5 \frac{-5 - 4N^2 + 6N^4}{(N^2 - 1)^2}$$

$$+ 8z^6 \frac{6 + 2N^2 - 5N^4}{(N^2 - 1)^2} + 4z^7 \frac{-32 - 42N^2 + 21N^4}{(N^2 - 1)^2} + 8z^8 \frac{184 + 98N^2 - 376N^4 + 203N^6 - 37N^8}{(N^2 - 4)(N^2 - 1)^3}$$

$$+ 2z^9 \frac{-6576 - 3656N^2 + 30\,629N^4 - 32\,810N^6 + 14\,735N^8 - 3245N^{10} + 275N^{12}}{(N^2 - 4)^2 (N^2 - 1)^4}$$

$$+ 8z^{10} \frac{4016 + 4136N^2 - 16\,789N^4 + 15\,608N^6 - 7937N^8 + 2257N^{10} - 238N^{12}}{(N^2 - 4)^2 (N^2 - 1)^4}$$

$$+ 2z^{11} (-34\,560 - 63\,904N^2 + 148\,416N^4 - 142\,210N^6$$
$$+ 74\,870N^8 - 19\,631N^{10} + 1658N^{12}) \frac{1}{(N^2 - 4)^2 (N^2 - 1)^4}$$

$$+ 8z^{12} (186\,048 + 87\,904N^2 - 727\,204N^4 + 1\,149\,812N^6$$
$$- 1\,175\,339N^8 + 716\,157N^{10} - 232\,150N^{12} + 34\,766N^{14} - 1906N^{16}) \frac{1}{(N^2 - 9)(N^2 - 4)^2 (N^2 - 1)^5}$$

$$+ 2z^{13} (-14\,774\,400 + 8\,055\,072N^2 + 58\,712\,088N^4$$
$$- 170\,052\,698N^6 + 261\,060\,513N^8 - 232\,073\,848N^{10} + 117\,200\,494N^{12}$$
$$- 33\,867\,953N^{14} + 5\,360\,045N^{16} - 433\,255N^{18} + 13\,878N^{20}) \frac{1}{(N^2 - 9)^2 (N^2 - 4)^2 (N^2 - 1)^6} + O(z^{14}), \tag{C15}$$

$$F = 2z^2 + 2z^4 + 4z^6 + z^8 \frac{14 - 30N^2 + 19N^4}{\left(N^2 - 1\right)^2} + 8z^{10} \frac{7 - 16N^2 + 12N^4}{\left(N^2 - 1\right)^2}$$

$$+ 2z^{12} \left(5952 - 30\,144\,N^2 + 63\,364\,N^4 - 67\,746\,N^6 + 37\,500\,N^8 - 9589\,N^{10} + 906\,N^{12}\right) \frac{1}{3\left(N^2 - 4\right)^2 \left(N^2 - 1\right)^4}$$

$$+ 4z^{14} \left(4704 - 25\,200\,N^2 + 55\,366\,N^4 - 62\,068\,N^6 + 36\,768\,N^8 - 10\,012\,N^{10} + 1009\,N^{12}\right) \frac{1}{\left(N^2 - 4\right)^2 \left(N^2 - 1\right)^4}$$

$$+ z^{16} \left(15\,230\,592 - 119\,651\,328\,N^2 + 409\,792\,072\,N^4\right.$$
$$- 799\,817\,292\,N^6 + 974\,422\,200\,N^8 - 760\,569\,676\,N^{10} + 375\,693\,595\,N^{12}$$
$$\left. - 112\,460\,534\,N^{14} + 19\,258\,826\,N^{16} - 1\,690\,814\,N^{18} + 58\,471\,N^{20}\right) \frac{1}{2\left(N^2 - 9\right)^2 \left(N^2 - 4\right)^2 \left(N^2 - 1\right)^6}$$

$$+ 8z^{18} \left(237\,447\,936 - 2\,045\,848\,320\,N^2 + 7\,796\,836\,128\,N^4\right.$$
$$- 17\,299\,894\,704\,N^6 + 24\,693\,730\,379\,N^8 - 23\,648\,019\,056\,N^{10} + 15\,403\,609\,647\,N^{12}$$
$$- 6\,787\,736\,700\,N^{14} + 1\,995\,934\,103\,N^{16} - 381\,749\,639\,N^{18} + 45\,159\,907\,N^{20}$$
$$\left. - 2\,974\,083\,N^{22} + 82\,898\,N^{24}\right) \frac{1}{3\left(N^2 - 9\right)^2 \left(N^2 - 4\right)^4 \left(N^2 - 1\right)^6} + O\!\left(z^{20}\right). \tag{C16}$$

APPENDIX D: THE GAUSSIAN MODEL ON THE HONEYCOMB LATTICE

There are a few subtleties in the analysis of models on the honeycomb lattice that are best illustrated by considering a simple Gaussian model of random walks. The essential point is related to the fact that lattice sites are not all related by a translation group: Only points at an even distance (in the number of lattice links) are related by such a symmetry. As a consequence, it is convenient to define even and odd fields ϕ_e, ϕ_o, according to the parity of the corresponding lattice sites with respect to an arbitrarily chosen origin, and even and odd correlation functions $G_e = \langle \phi_e \phi_e \rangle = \langle \phi_o \phi_o \rangle$, $G_o = \langle \phi_e \phi_o \rangle = \langle \phi_o \phi_e \rangle$.

Let us represent the Cartesian coordinates of the (finite, periodic) lattice sites by

$$(x,y)_e = \left(\tfrac{3}{2}m, \tfrac{1}{2}\sqrt{3}n\right) a, \tag{D1a}$$

$$(x,y)_o = \left(\tfrac{3}{2}m + 1, \tfrac{1}{2}\sqrt{3}n\right) a, \tag{D1b}$$

where m and n are integer numbers satisfying the conditions $0 \le m < L_1$, $0 \le n < 2L_2$, and $m + n$ is even. The total number of lattice points is $2L_1 \times L_2$, the number of links is $3L_1 \times L_2$, and the number of plaquettes is $L_1 \times L_2$.

The finite-lattice Fourier transform is consistently defined by

$$G_e(p) = \sum_{x \text{ even}} e^{ip \cdot x} G_e(x) \tag{D2}$$

and similarly for $G_o(p)$; the set of momenta is

$$p = \frac{2\pi}{a} \left(\frac{2}{3}\frac{\tilde{m}}{L_1}, \frac{1}{\sqrt{3}}\frac{\tilde{n}}{L_2}\right), \tag{D3}$$

with $\tilde{m}$ and $\tilde{n}$ integers, and $0 \le \tilde{m} < L_1$, $0 \le \tilde{n} < L_2$.

In a random walk model where walks of length ν are weighted by a factor β^ν, it is easy to establish from the recursion relations the relationships

$$G_e(p) = \beta e^{-ip_1} \left[1 + 2\cos \tfrac{1}{2}\sqrt{3}p_2 \, e^{3ip_1/2}\right] G_o(p) + 1, \tag{D4a}$$

$$G_o(p) = \beta e^{ip_1} \left[1 + 2\cos \tfrac{1}{2}\sqrt{3}p_2 \, e^{-3ip_1/2}\right] G_e(p), \tag{D4b}$$

where $G_e(p)$ and $G_o(p)$ are the Fourier transform of $G_e(x)$ and $G_o(x)$, respectively. As a consequence, we obtain the even momentum-space Green's functions in the form

$$G_e(p)$$
$$= \frac{1}{1 - \beta^2 \left[1 + 4\cos^2 \tfrac{1}{2}\sqrt{3}p_2 + 4\cos \tfrac{1}{2}\sqrt{3}p_2 \cos \tfrac{3}{2}p_1\right]}. \tag{D5}$$

The critical value of β is easily found to be $\beta_c = \tfrac{1}{3}$, and as a consequence we find the massless lattice (even) propagator

$$\Delta_e(p) = \frac{9}{8 - 4\cos^2 \tfrac{1}{2}\sqrt{3}p_2 + 4\cos \tfrac{1}{2}\sqrt{3}p_2 \cos \tfrac{3}{2}p_1}$$
$$\xrightarrow{p \to 0} \frac{2}{p^2}. \tag{D6}$$

The odd propagator is simply

$$\Delta_o(p) = \tfrac{1}{3}e^{ip_1} \left[1 + 2\cos \tfrac{1}{2}\sqrt{3}p_2 \, e^{-3ip_1/2}\right] \Delta_e(p). \tag{D7}$$

The structure of the propagator in the Gaussian model offers an important indication about the possibility of exponentiation in wall-wall correlations. Let us indeed recall that exponentiation corresponds to a simple structure

$$\frac{1}{A - B\cos p} \tag{D8}$$

in the corresponding propagator. Let us now observe that Eq. (D5) implies

$$G_e(p_1, 0) = \frac{1}{1 - \beta^2 \left[5 + 4 \cos \frac{3}{2} p_1\right]}, \qquad \text{(D9)}$$

$$G_e(0, p_2) + G_o(0, p_2) = \frac{1}{1 - \beta \left[1 + 2 \cos \frac{1}{2} \sqrt{3} p_2\right]}. \qquad \text{(D10)}$$

We have therefore the possibility of defining two different exponentiated "wall-wall" correlation functions: i.e.,

$$G_1^{(w)}(x) = \sum_y G_e(x, y), \qquad \text{(D11)}$$

$$G_2^{(w)}(x) = \sum_y \left[G_e(x, y) + G_o(x, y)\right]. \qquad \text{(D12)}$$

Even in more general models, in the strong-coupling domain, for a sufficiently large lattice distance exponentiation will hold for the correlation functions $G_1^{(w)}(x)$ and $G_2^{(w)}(x)$. If we take into account the discrete rotational

symmetry of the honeycomb lattice, we may easily recognize that the above correlations can be referred to directions differing by a $\pi/6$ angle, and this is the maximal violation of the full rotational symmetry one can find on this kind of lattice. Therefore the ratio of the two different correlation lengths one may define is an optimal measurement of the violation of rotational invariance in the model under examination, in analogy with the side/diagonal mass ratio of the square lattice.

APPENDIX E: HONEYCOMB-LATTICE RESULTS FOR FINITE N

We list in the present appendix the values of the quantities defined in Sec. IX without further comments. The definition of these quantities presented here is discussed in Sec. IX:

$$
\begin{aligned}
\mu_1 = \frac{2}{3} \Bigg[&-\ln 2z^2 - z^2 - \frac{1}{2} z^4 + z^6 \frac{-14 + 46\,N^2 - 41\,N^4}{6\left(N^2 - 1\right)^2} + z^8 \frac{9 - 27\,N^2 + 35\,N^4 - 37\,N^6}{4\left(N^2 - 1\right)^3} \\
&+ z^{10} \frac{-194 + 1136\,N^2 - 2539\,N^4 + 2546\,N^6 - 1174\,N^8}{20\left(N^2 - 1\right)^4} \\
&+ z^{12} \big(-6208 + 49\,952\,N^2 - 175\,780\,N^4 + 360\,896\,N^6 - 469\,546\,N^8 \\
&\quad + 395\,168\,N^{10} - 205\,477\,N^{12} + 56\,246\,N^{14} - 6169\,N^{16}\big) \frac{1}{24\left(N^2 - 4\right)^2 \left(N^2 - 1\right)^6} \\
&+ z^{14} \big(-204\,800 + 2\,013\,696\,N^2 - 8\,684\,352\,N^4 + 21\,407\,856\,N^6 \\
&\quad - 33\,518\,156\,N^8 + 34\,888\,595\,N^{10} - 24\,526\,859\,N^{12} + 11\,475\,108\,N^{14} \\
&\quad - 3\,337\,802\,N^{16} + 545\,557\,N^{18} - 39\,943\,N^{20}\big) \frac{1}{56\left(N^2 - 4\right)^3 \left(N^2 - 1\right)^7} \\
&+ z^{16} \big(-253\,184 + 2\,885\,888\,N^2 - 14\,879\,968\,N^4 + 46\,028\,112\,N^6 \\
&\quad - 95\,149\,021\,N^8 + 138\,282\,732\,N^{10} - 144\,193\,790\,N^{12} + 108\,442\,897\,N^{14} \\
&\quad - 58\,120\,117\,N^{16} + 21\,234\,008\,N^{18} - 4\,926\,461\,N^{20} + 646\,061\,N^{22} - 36\,361\,N^{24}\big) \\
&\times \frac{1}{8\left(N^2 - 4\right)^4 \left(N^2 - 1\right)^8} \Bigg] + O\!\left(z^{18}\right),
\end{aligned}
\qquad \text{(E1)}
$$

$$
\begin{aligned}
\mu_2 = \frac{2}{3}\sqrt{3} \Bigg[&-\ln z - z + \frac{1}{2} z^2 - \frac{1}{3} z^3 - \frac{3}{4} z^4 - \frac{1}{5} z^5 - z^6 \frac{1 + 11\,N^2}{6\left(N^2 - 1\right)} \\
&+ 2z^7 \frac{-4 + N^2 - 18\,N^4}{7\left(N^2 - 1\right)^2} + z^8 \frac{11 - 81\,N^2 + N^4 + 29\,N^6}{8\left(N^2 - 1\right)^3} + 5z^9 \frac{2 + 12\,N^2 + 24\,N^4 - 11\,N^6}{9\left(N^2 - 1\right)^3} \\
&+ z^{10} \frac{19 - 277\,N^2 + 127\,N^4 - 319\,N^6}{10\left(N^2 - 1\right)^3} + z^{11} \frac{-34 + 26\,N^2 - 622\,N^4 + 587\,N^6 - 452\,N^8}{11\left(N^2 - 1\right)^4} \\
&+ z^{12} \frac{-132 + 1045\,N^2 - 1813\,N^4 + 2158\,N^6 - 558\,N^8 - 115\,N^{10} - 69\,N^{12}}{4\left(N^2 - 4\right)\left(N^2 - 1\right)^5} \\
&+ z^{13} \big(-1472 + 5408\,N^2 - 24\,716\,N^4 + 48\,156\,N^6 - 97\,577\,N^8 \\
&\quad + 118\,419\,N^{10} - 65\,911\,N^{12} + 18\,318\,N^{14} - 2614\,N^{16}\big) \frac{1}{13\left(N^2 - 4\right)^2 \left(N^2 - 1\right)^6} \\
&+ z^{14} \big(5568 - 91\,344\,N^2 + 393\,204\,N^4 - 964\,687\,N^6 + 1\,168\,570\,N^8 \\
&\quad - 845\,302\,N^{10} + 432\,359\,N^{12} - 133\,335\,N^{14} + 18\,275\,N^{16} - 885\,N^{18}\big) \frac{1}{7\left(N^2 - 4\right)^3 \left(N^2 - 1\right)^6}
\end{aligned}
$$

$$
\begin{aligned}
&+ z^{15}\left(-25\,024 + 122\,896\,N^2 - 380\,772\,N^4 + 569\,163\,N^6 - 1\,634\,619\,N^8\right.\\
&\qquad \left. + 3\,326\,040\,N^{10} - 3\,347\,466\,N^{12} + 1\,923\,822\,N^{14} - 642\,978\,N^{16} + 116\,764\,N^{18} - 7576\,N^{20}\right)\\
&\qquad \times \frac{1}{15\left(N^2-4\right)^3\left(N^2-1\right)^7}\\
&+ z^{16}\left(43\,712 - 656\,912\,N^2 + 3\,472\,772\,N^4 - 10\,632\,331\,N^6\right.\\
&\qquad + 18\,690\,504\,N^8 - 20\,221\,284\,N^{10} + 15\,125\,616\,N^{12} - 8\,770\,834\,N^{14} + 4\,069\,272\,N^{16}\\
&\qquad \left. - 1\,342\,540\,N^{18} + 260\,364\,N^{20} - 24\,083\,N^{22}\right)\frac{1}{16\left(N^2-4\right)^3\left(N^2-1\right)^8}\Bigg] + O\!\left(z^{17}\right),
\end{aligned}
\tag{E2}
$$

$$
\begin{aligned}
\chi =\ & 1 + 3\,z + 6\,z^2 + 12\,z^3 + 24\,z^4 + 48\,z^5 + 90\,z^6 + 174\,z^7 + 12\,z^8\,\frac{-28 + 29\,N^2}{N^2-1} + 18\,z^9\,\frac{36 - 74\,N^2 + 39\,N^4}{\left(N^2-1\right)^2}\\
&+ 6\,z^{10}\,\frac{-203 + 625\,N^2 - 649\,N^4 + 232\,N^6}{\left(N^2-1\right)^3} + 6\,z^{11}\,\frac{388 - 1592\,N^2 + 2469\,N^4 - 1725\,N^6 + 469\,N^8}{\left(N^2-1\right)^4}\\
&+ 6\,z^{12}\,\frac{736 - 3056\,N^2 + 4802\,N^4 - 3407\,N^6 + 943\,N^8}{\left(N^2-1\right)^4}\\
&+ 6\,z^{13}\,\frac{1398 - 5850\,N^2 + 9318\,N^4 - 6743\,N^6 + 1922\,N^8}{\left(N^2-1\right)^4}\\
&+ 6\,z^{14}\,\frac{-10\,520 + 47\,078\,N^2 - 82\,728\,N^4 + 70\,812\,N^6 - 28\,891\,N^8 + 3951\,N^{10}}{\left(N^2-4\right)\left(N^2-1\right)^4}\\
&+ 6\,z^{15}\left(79\,712 - 380\,208\,N^2 + 730\,934\,N^4 - 716\,200\,N^6 + 372\,088\,N^8 - 91\,009\,N^{10} + 8228\,N^{12}\right)\\
&\qquad \times \frac{1}{\left(N^2-4\right)^2\left(N^2-1\right)^4}\\
&+ 6\,z^{16}\left(600\,192 - 3\,641\,312\,N^2 + 9\,388\,472\,N^4 - 13\,344\,618\,N^6\right.\\
&\qquad \left. + 11\,337\,734\,N^8 - 5\,813\,592\,N^{10} + 1\,719\,475\,N^{12} - 267\,280\,N^{14} + 16\,906\,N^{16}\right)\frac{1}{\left(N^2-4\right)^3\left(N^2-1\right)^5}\\
&+ 6\,z^{17}\left(4\,531\,200 - 33\,355\,776\,N^2 + 107\,774\,336\,N^4\right.\\
&\qquad - 200\,423\,616\,N^6 + 236\,373\,604\,N^8 - 183\,407\,604\,N^{10} + 93\,969\,088\,N^{12}\\
&\qquad \left. - 31\,097\,639\,N^{14} + 6\,341\,524\,N^{16} - 722\,188\,N^{18} + 35\,215\,N^{20}\right)\frac{1}{\left(N^2-4\right)^4\left(N^2-1\right)^6}\\
&+ 6\,z^{18}\left(-8\,505\,600 + 71\,553\,024\,N^2 - 268\,314\,976\,N^4\right.\\
&\qquad + 590\,267\,696\,N^6 - 843\,497\,305\,N^8 + 818\,280\,951\,N^{10} - 546\,354\,607\,N^{12}\\
&\qquad \left. + 249\,146\,769\,N^{14} - 75\,461\,014\,N^{16} + 14\,404\,142\,N^{18} - 1\,562\,138\,N^{20} + 73\,433\,N^{22}\right)\frac{1}{\left(N^2-4\right)^4\left(N^2-1\right)^7}\\
&+ 6\,z^{19}\left(16\,021\,504 - 151\,615\,488\,N^2 + 647\,496\,704\,N^4\right.\\
&\qquad - 1\,646\,428\,032\,N^6 + 2\,769\,093\,400\,N^8 - 3\,234\,820\,688\,N^{10} + 2\,679\,887\,383\,N^{12}\\
&\qquad - 1\,577\,573\,745\,N^{14} + 650\,694\,030\,N^{16} - 182\,224\,525\,N^{18} + 32\,769\,509\,N^{20}\\
&\qquad \left. - 3\,399\,903\,N^{22} + 154\,769\,N^{24}\right)\frac{1}{\left(N^2-4\right)^4\left(N^2-1\right)^8}\\
&+ 6\,z^{20}\left(-270\,452\,736 + 2\,603\,295\,744\,N^2 - 11\,339\,998\,976\,N^4\right.\\
&\qquad + 29\,517\,395\,456\,N^6 - 51\,057\,737\,736\,N^8 + 61\,725\,236\,828\,N^{10} - 53\,378\,649\,928\,N^{12}\\
&\qquad + 33\,218\,024\,089\,N^{14} - 14\,765\,553\,520\,N^{16} + 4\,594\,385\,593\,N^{18} - 966\,784\,918\,N^{20}\\
&\qquad \left. + 129\,788\,872\,N^{22} - 9\,932\,849\,N^{24} + 325\,065\,N^{26}\right)\frac{1}{\left(N^2-9\right)\left(N^2-4\right)^4\left(N^2-1\right)^8} + O\!\left(z^{21}\right),
\end{aligned}
\tag{E3}
$$

$$M_G^2 = \tfrac{4}{3} z^{-1} - 4 + \tfrac{8}{3} z - 8 z^6 \frac{N^2 + 1}{N^2 - 1} + 8 z^7 \frac{-7 - 10 N^2 + 5 N^4}{3 \left(N^2 - 1\right)^2}$$

$$+ 8 z^8 \frac{-3 - 7 N^2 + 4 N^4 + N^6}{\left(N^2 - 1\right)^3} + 8 z^9 \frac{-12 - 20 N^2 + 29 N^6 - 6 N^8}{3 \left(N^2 - 1\right)^4}$$

$$+ 8 z^{10} \frac{12 - 6 N^2 + 15 N^4 + 8 N^6 - 11 N^8}{\left(N^2 - 1\right)^4} + 8 z^{11} \frac{-82 - 34 N^2 + 165 N^4 - 247 N^6 + 36 N^8}{3 \left(N^2 - 1\right)^4}$$

$$+ 8 z^{12} \frac{-160 - 432 N^2 + 698 N^4 - 409 N^6 - 2 N^8 - 18 N^{10}}{\left(N^2 - 4\right) \left(N^2 - 1\right)^4}$$

$$+ 8 z^{13} \frac{-1776 - 12\,392 N^2 + 3665 N^4 + 1850 N^6 - 1811 N^8 - 666 N^{10} + 73 N^{12}}{3 \left(N^2 - 4\right)^2 \left(N^2 - 1\right)^4}$$

$$+ 8 z^{14} \left(3328 + 9920 N^2 + 23\,760 N^4 - 41\,452 N^6 + 12\,242 N^8 \right.$$
$$\left. + 5969 N^{10} - 5077 N^{12} + 657 N^{14} - 5 N^{16}\right) \frac{1}{\left(N^2 - 4\right)^3 \left(N^2 - 1\right)^5}$$

$$+ 8 z^{15} \left(-114\,432 + 400\,128 N^2 - 1\,536\,160 N^4 + 1\,733\,488 N^6 \right.$$
$$- 323\,935 N^8 - 602\,516 N^{10} + 449\,683 N^{12} - 124\,964 N^{14} + 5895 N^{16}$$
$$\left. + 1675 N^{18} - 75 N^{20}\right) \frac{1}{3 \left(N^2 - 4\right)^4 \left(N^2 - 1\right)^6}$$

$$+ 8 z^{16} \left(-91\,136 + 441\,856 N^2 - 1\,078\,144 N^4 + 768\,256 N^6 \right.$$
$$+ 450\,812 N^8 - 1\,054\,246 N^{10} + 839\,396 N^{12} - 464\,465 N^{14} + 194\,981 N^{16}$$
$$\left. - 54\,586 N^{18} + 9491 N^{20} - 690 N^{22}\right) \frac{1}{\left(N^2 - 4\right)^4 \left(N^2 - 1\right)^7}$$

$$+ 8 z^{17} \left(-425\,728 + 1\,766\,144 N^2 - 1\,985\,440 N^4 - 5\,221\,520 N^6 \right.$$
$$+ 17\,290\,561 N^8 - 24\,613\,836 N^{10} + 24\,266\,712 N^{12} - 17\,725\,908 N^{14}$$
$$\left. + 9\,035\,120 N^{16} - 2\,989\,557 N^{18} + 594\,069 N^{20} - 63\,766 N^{22} + 2193 N^{24}\right) \frac{1}{3 \left(N^2 - 4\right)^4 \left(N^2 - 1\right)^8}$$

$$+ 8 z^{18} \left(-1\,661\,184 + 3\,794\,944 N^2 + 7\,844\,000 N^4 \right.$$
$$- 54\,955\,728 N^6 + 119\,244\,695 N^8 - 171\,667\,137 N^{10} + 175\,851\,305 N^{12}$$
$$- 120\,836\,371 N^{14} + 53\,853\,632 N^{16} - 15\,114\,634 N^{18} + 2\,512\,157 N^{20}$$
$$\left. - 229\,837 N^{22} + 9716 N^{24} - 526 N^{26}\right) \frac{1}{\left(N^2 - 9\right) \left(N^2 - 4\right)^4 \left(N^2 - 1\right)^8} + O\!\left(z^{19}\right), \tag{E4}$$

$$F = \tfrac{3}{2} z^2 + z^6 + 3 z^{10} + z^{12} \frac{4 - 18 N^2 + 32 N^4 - 27 N^6 + 18 N^8}{2 \left(N^2 - 1\right)^4} + 12 z^{14}$$

$$+ 6 z^{16} \frac{3 - 16 N^2 + 32 N^4 - 29 N^6 + 19 N^8}{\left(N^2 - 1\right)^4}$$

$$+ z^{18} \left(49\,920 - 268\,032 N^2 + 595\,744 N^4 - 732\,080 N^6 \right.$$
$$\left. + 536\,515 N^8 - 239\,924 N^{10} + 65\,162 N^{12} - 10\,174 N^{14} + 829 N^{16}\right) \frac{1}{3 \left(N^2 - 4\right)^4 \left(N^2 - 1\right)^4}$$

$$+ 3 z^{20} \left(92 - 890 N^2 + 3756 N^4 - 9052 N^6 + 13\,836 N^8 \right.$$
$$\left. - 14\,023 N^{10} + 9380 N^{12} - 3690 N^{14} + 720 N^{16}\right) \frac{1}{2 \left(N^2 - 1\right)^8}$$

$$+ 3 z^{22} \left(36\,864 - 368\,640 N^2 + 1\,666\,560 N^4 - 4\,505\,344 N^6 \right.$$
$$+ 8\,111\,248 N^8 - 10\,267\,152 N^{10} + 9\,373\,736 N^{12} - 6\,230\,112 N^{14}$$
$$\left. + 3\,011\,024 N^{16} - 1\,020\,866 N^{18} + 227\,573 N^{20} - 30\,248 N^{22} + 1918 N^{24}\right) \frac{1}{\left(N^2 - 4\right)^4 \left(N^2 - 1\right)^8}$$

$$+ z^{24} \left(7\,215\,630\,336 - 96\,566\,722\,560 N^2 + 592\,839\,316\,224 N^4 \right.$$

$$
\begin{aligned}
&- 2\,214\,635\,962\,752\,N^6 + 5\,639\,017\,965\,384\,N^8 - 10\,385\,973\,650\,808\,N^{10} \\
&+ 14\,322\,131\,449\,584\,N^{12} - 15\,072\,994\,434\,276\,N^{14} + 12\,212\,762\,091\,344\,N^{16} \\
&- 7\,627\,059\,006\,688\,N^{18} + 3\,656\,946\,091\,530\,N^{20} - 1\,335\,009\,872\,497\,N^{22} \\
&+ 366\,664\,198\,242\,N^{24} - 74\,601\,540\,139\,N^{26} + 11\,013\,519\,148\,N^{28} - 1\,144\,634\,371\,N^{30} \\
&+ 79\,672\,354\,N^{32} - 3\,373\,733\,N^{34} + 68\,030\,N^{36}\Big) \frac{1}{4\left(N^2-9\right)^4\left(N^2-4\right)^4\left(N^2-1\right)^{10}} \\[2mm]
&+ 3\,z^{26}\Big(-275\,712 + 3\,201\,536\,N^2 - 17\,022\,176\,N^4 \\
&+ 54\,825\,776\,N^6 - 119\,171\,333\,N^8 + 184\,722\,213\,N^{10} - 210\,428\,660\,N^{12} \\
&+ 178\,609\,366\,N^{14} - 112\,928\,266\,N^{16} + 52\,388\,456\,N^{18} - 17\,133\,329\,N^{20} \\
&+ 3\,699\,171\,N^{22} - 474\,540\,N^{24} + 29\,132\,N^{26}\Big) \frac{1}{\left(N^2-4\right)^4\left(N^2-1\right)^9} + O\!\left(z^{28}\right).
\end{aligned}
\tag{E5}
$$

[1] F. Green and S. Samuel, Nucl. Phys. **B190**, 113 (1981).
[2] F. Green and S. Samuel, Phys. Lett. **103B**, 110 (1981).
[3] F. Green and S. Samuel, Nucl. Phys. **B194**, 107 (1982).
[4] P. Rossi and E. Vicari, Phys. Rev. D **49**, 1621 (1994).
[5] P. Rossi and E. Vicari, Phys. Rev. D **49**, 6072 (1994); **50**, 4718(E) (1994).
[6] M. Campostrini, P. Rossi, and E. Vicari, Phys. Rev. D **51**, 958 (1995).
[7] M. R. Douglas and S. H. Shenker, Nucl. Phys. **B335**, 635 (1990).
[8] D. J. Gross and A. A. Migdal, Phys. Rev. Lett. **64**, 127 (1990).
[9] E. Brezin and V. A. Kazakov, Phys. Lett. B **236**, 144 (1990).
[10] V. Periwal and D. Shevitz, Phys. Rev. Lett. **64**, 1326 (1990).
[11] J.-M. Drouffe and J.-B. Zuber, Phys. Rep. **102**, 1 (1983).
[12] E. Rabinovici and S. Samuel, Phys. Lett. **101B**, 323 (1981).
[13] G. Parisi, *Statistical Field Theory* (Addison-Wesley, Redwood City, CA, 1988).
[14] C. Itzykson and J.-M. Drouffe, *Statistical Field Theory* (Cambridge University Press, Cambridge, England, 1989).
[15] B. de Wit and G. 't Hooft, Phys. Lett. **69B**, 61 (1977).
[16] R. C. Brower, P. Rossi, and C.-I. Tan, Phys. Rev. D **23**, 942 (1981).
[17] R. C. Brower, P. Rossi, and C.-I. Tan, Phys. Rev. D **23**, 953 (1981).